



EUROPEAN LABORATORY FOR PARTICLE PHYSICS

CERN-PPE/92-30
13 February 1992

Physics and Design of the Tau-Charm Factory in Spain

Jasper Kirkby

CERN, Geneva, Switzerland

Abstract

We describe the physics prospects of the τ -charm Factory—a high-luminosity e^+e^- collider operating near τ and charm thresholds—and summarize the design of the Spanish τ -charm Factory project.

Presented at the
International Workshop on Electroweak Physics
Beyond the Standard Model,
Valencia, Spain, 2-5 October 1991

Physics and Design of the Tau-Charm Factory in Spain

Jasper Kirkby

CERN, Geneva, Switzerland

Abstract

We describe the physics prospects of the τ -charm Factory—a high-luminosity e^+e^- collider operating near τ and charm thresholds—and summarize the design of the Spanish τ -charm Factory project.

1 Introduction

1.1 Progress of particle physics in Europe

The development of particle physics over the last two decades has been one of remarkable success. The “Standard Model” of weak, electromagnetic and strong interactions has accommodated or predicted every single confirmed experimental result. But this does not mean that the search is over; the Standard Model leaves many fundamental questions unanswered, and it lacks the simplicity of the ultimate truth. We do not know, for example, the principle that determines what the elementary particles and fundamental forces must be. Nor do we understand the mechanism that gives each particle-type its own mass.

Historically, decisive progress in particle physics has occurred along two complementary lines:

1. The discovery of new particles and interactions at the “high-energy frontier”.
2. The detailed study of the known particles and forces at the “high-precision frontier”.

There have been many important discoveries along the first line, of which the two first neutrino types (ν_e and ν_μ), the J/ψ resonance, and the W^\pm and Z^0 bosons are examples. Similarly, there have been many important high-precision experiments such as those measuring the CP violation parameters in K^0 decay, the anomalous magnetic moment of e 's and μ 's, rare K decays, and the mass and couplings of the Z^0 .

The European particle-physics programme has evolved along these two lines: on the one hand, low energy but relatively-precise experiments at fixed-target machines and at electron-positron colliders such as ADONE, ACO, DORIS and PETRA and, on the other hand, high-energy but generally less-precise experiments at hadron colliders such as the ISR and SPS Collider. LEP currently enjoys the privileged position of being at both the high-energy and high-precision frontiers simultaneously. Experience has confirmed the importance of pursuing several complementary approaches in parallel since the basic subatomic phenomena can only be unravelled from a broad experimental basis; witness the development of the Standard Model, whose empirical basis covers the entire body of particle physics data. In

order to proceed beyond the current orthodoxy, a rich and varied set of constraints will no doubt again play a fundamental role. Considerations such as these have led to a broad experimental programme in Europe—a diversity which Europe should seek to maintain in the future.

With the LEP constraint of precisely three light-neutrino types, only the t quark and the elementary Higgs scalar(s) remain to be found to complete the spectrum of the “minimal” Standard Model. The observation that Nature appears to have only three families of fundamental fermions— $[(\nu_e, e)(u, d)]$, $[(\nu_\mu, \mu)(c, s)]$, and $[(\nu_\tau, \tau)(t, b)]$ —has underscored the importance of precise studies of these particles in search of clues towards further progress.

In Europe, the near-future strategy for exploring the high-energy frontier is centred on the LEP-LHC complex at CERN, and on HERA at DESY. A major motivation for these machines is to discover the missing particles of the Standard Model. But even the discoveries of the t quark and the Higgs scalar would not solve major puzzles such as the reasons for the existence of three families and the mass-values themselves. CERN is also well-placed to deepen the exploration of the fundamental vector bosons with LEP and HLEP (a Z^0 factory, with a tenfold luminosity upgrade).

Among the known fermions, there are four about which we have much more to learn: the τ and ν_τ leptons, and the c and b quarks. Studies of the b quark will be made at the proposed B factories, as well at LEP and at the LHC. In addition, further progress in the studies of the lighter quarks and leptons will be made by machines such as the ϕ factory at Frascati (DAΦNE) and the KAON factory at TRIUMF.

The purpose of the τ -charm Factory is to enable precise studies to be made of three of the poorly-known fermions: the τ , ν_τ and c . The objective is to measure the properties of these particles with precisions comparable to our present knowledge of the lighter quarks and leptons. This would provide us with precious information on the flavour structure of the theory, especially since it is expected that the heavier flavours will be more sensitive to physics beyond the Standard Model. Of particular interest is the τ : a third generation, massive lepton which has a wide variety of decay channels, both leptonic and hadronic, that are calculated with high precision in the Standard Model. As for the c quark, it is the only heavy up-type quark that is accessible to precision experiments. In addition to direct studies, the c quark also provides—through decays of the J/ψ —an ideal tool for light meson and gluonium spectroscopy and for precise tests of symmetry principles.

The original concept of the τ -charm Factory[1, 2, 3] involves an integrated detector and e^+e^- collider operating in the centre-of-mass energy range 3.0-5.0 GeV. The peak luminosity of the collider, $10^{33} \text{ cm}^{-2}\text{sec}^{-1}$, represents an improvement by 2-3 orders of magnitude over previous machines at these energies (Fig. 1).

Spain has recently proposed to build a τ -charm Factory in a new laboratory, and has offered to provide the major fraction of the funds. Since Spain has never had a national accelerator programme, it is seeking collaboration with CERN on the project. Although particle factories are within the range of national research funds, they are nevertheless technically challenging and require a high level of machine expertise, such as found at CERN. Particle factories are an important part of the future European High Energy Physics Programme and the Spanish initiative represents a special opportunity for Europe to build a τ -charm Factory.

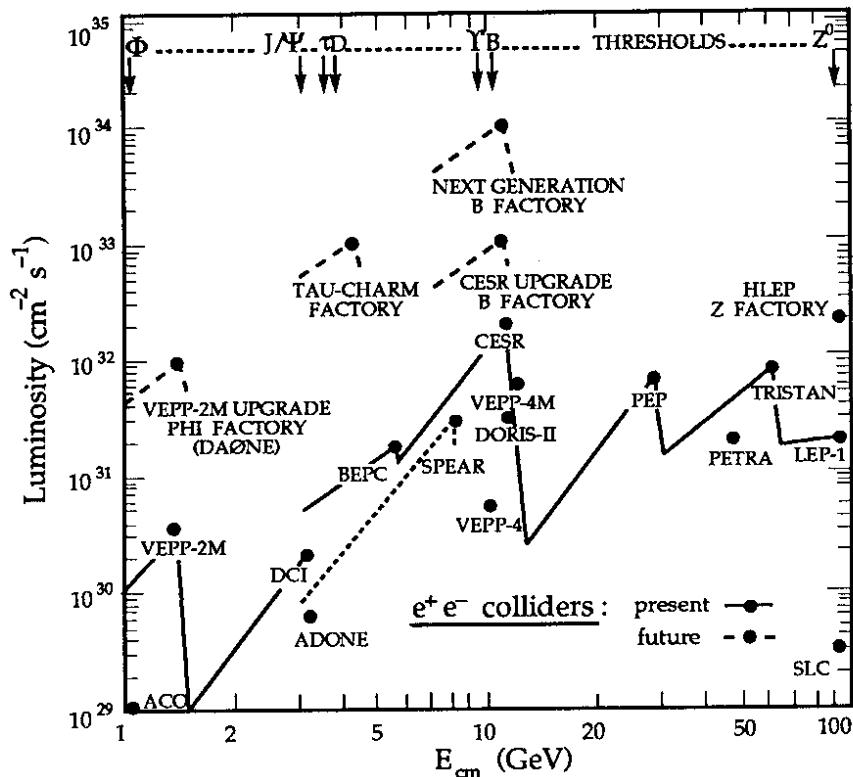


Figure 1: The luminosity of present and future e^+e^- colliders in the centre-of-mass energy range $1 \leq E_{cm} \leq 100$ GeV. The solid line represents the present envelope of the maximum luminosity. The long-dashed lines indicate the design luminosities of future factories. The short-dashed line shows the previous (SPEAR) luminosity in the $\tau^+\tau^-$ threshold region.

1.2 The next step in experimental sensitivity

Substantial progress in the understanding of the τ lepton and charm quark will require future experiments with the following characteristics:

	Present experiments	→	Future experiments
Increased statistics	$10^5 - 10^6$		$\approx 10^8$
Reduced backgrounds	1-10%		$\lesssim 0.1\%$
Reduced systematic errors	1-10%		$\approx 0.1\%$

Present measurements have been by-products of experiments with other primary goals. Systematic precisions of a few per cent have been achieved, which have largely been adequate in view of the available statistics. However, with the sharp increase in statistics that is foreseen in this next step, backgrounds and systematic errors are likely to dominate the precisions of future measurements. Although there are several prospective e^+e^- colliders that would generate copious data samples of τ and charm particles, the best place to achieve the required systematic precision is a dedicated machine operating near τ and charm thresholds.

While the τ lepton was discovered[4] near threshold, most of the recent experimental advances have been made at higher energies, reflecting increased statistics and reduced back-

grounds relative to the pioneer experiments. In this historical light, it is instructive first to review the special advantages of the threshold region which provide the τ -charm Factory with a unique experimental environment for τ and charm studies. These are presented in the next section, followed by a discussion of the physics highlights. Finally, we summarize the design of the Spanish τ -charm Factory.

Many of the results presented here have emerged from recent workshops at SLAC[5], Orsay[6], Sevilla[7] and CERN[8]. Further details, as well as a complete list of references, can be found in the Proceedings of these meetings. In addition, excellent reviews of the status of τ physics and of the charm physics potential of a τ -charm Factory can be found in refs. [9] and [10], respectively.

2 Experimental advantages of the τ -charm threshold region

The energy range of the τ -charm Factory embraces three important thresholds: those for the τ lepton, the D mesons, and the J/ψ and other charmonium states. As a result, the τ -charm Factory can answer an exceptionally broad range of fundamental questions facing the Standard Model, and at the same time explore the frontier of its possible extensions.

The advantages of a τ -charm Factory involve not only the very large data samples but also an excellent control of systematic errors, resulting from a unique experimental environment that includes the following:

- Exceptionally-low backgrounds, which can be measured experimentally.
- τ leptons and D mesons are produced nearly at rest, and so many of the decays are separated kinematically, e.g. two-body decays yield monochromatic particles.
- τ leptons can be single-tagged since they are produced below the threshold for b and c production. In addition, each of the D mesons— D^0 , D^\pm and D_s^\pm —can be single-tagged.

These and other advantages are discussed in more detail in the remainder of this section.

2.1 Statistics and operating points

A comparison of the yearly data samples from a τ -charm Factory, a B Factory and a Z Factory is shown in Table 1. Although the highest cross-sections for $\tau^+\tau^-$ and $c\bar{c}$ occur near threshold, each of these machines will produce copious data samples and, on purely statistical grounds, the differences between the machines are not very large. Of greater significance, however, and what makes the τ -charm Factory the best experimental tool for τ and charm physics, is its control of systematic errors. This is due to the presence of several operating points (see Figs. 2 and 3) with unique properties:

- $J/\psi(3.10)$. The J/ψ provides an intense and clean source of light hadrons and gluonic particles for QCD studies and for tests of symmetry principles. In addition, it provides a high-rate ($\simeq 1$ kHz) signal for calibration and monitoring of the detector performance.
- **3.56 GeV**. This energy, which is just below $\tau^+\tau^-$ threshold (assuming the present value of the τ mass: 1784^{+3}_{-4} MeV/ c^2), provides experimental measurement of all non- τ backgrounds: hadronic ($u\bar{u}$, $d\bar{d}$ and $s\bar{s}$), two-photon, QED ($e\bar{e}(\gamma)$, $\mu\bar{\mu}(\gamma)$, etc.) and beam gas.

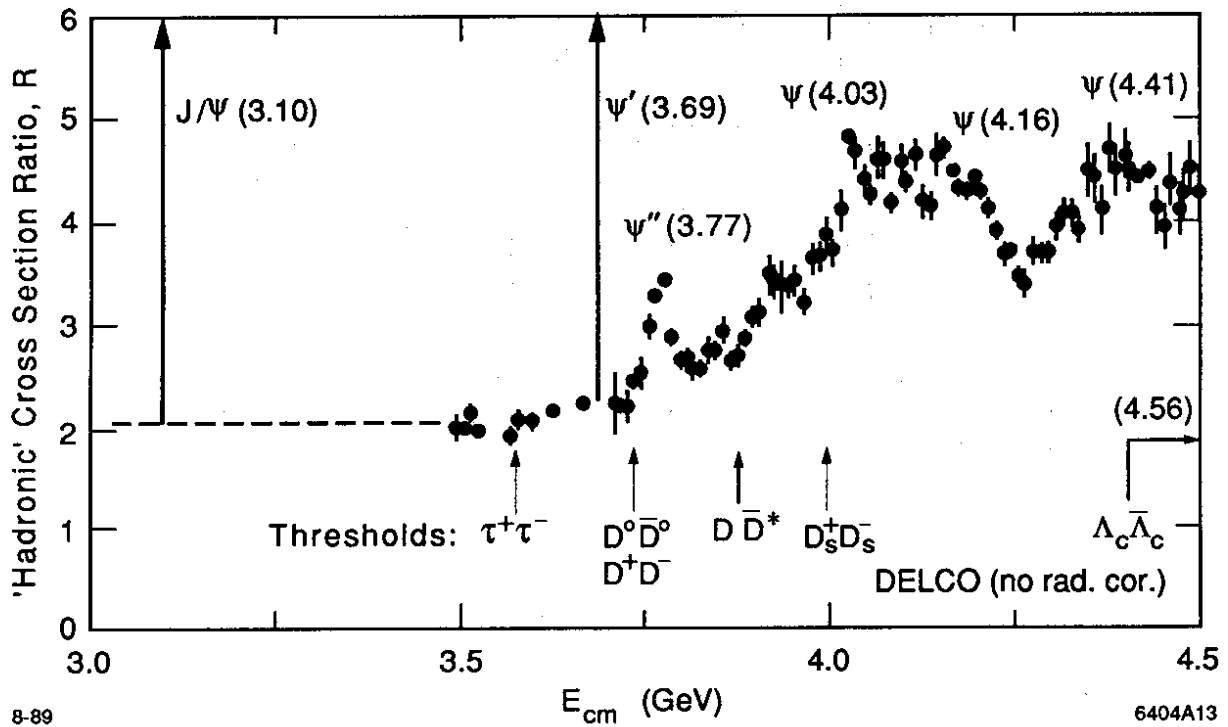


Figure 2: The energy range of the τ -charm Factory. The ratio $R = \sigma(e^+e^- \rightarrow \text{'hadrons'}) / \sigma(e^+e^- \rightarrow \mu^+\mu^-)$, where 'hadrons' include both $q\bar{q}$ and $\tau^+\tau^-$ events. The data are from DELCO at SPEAR.

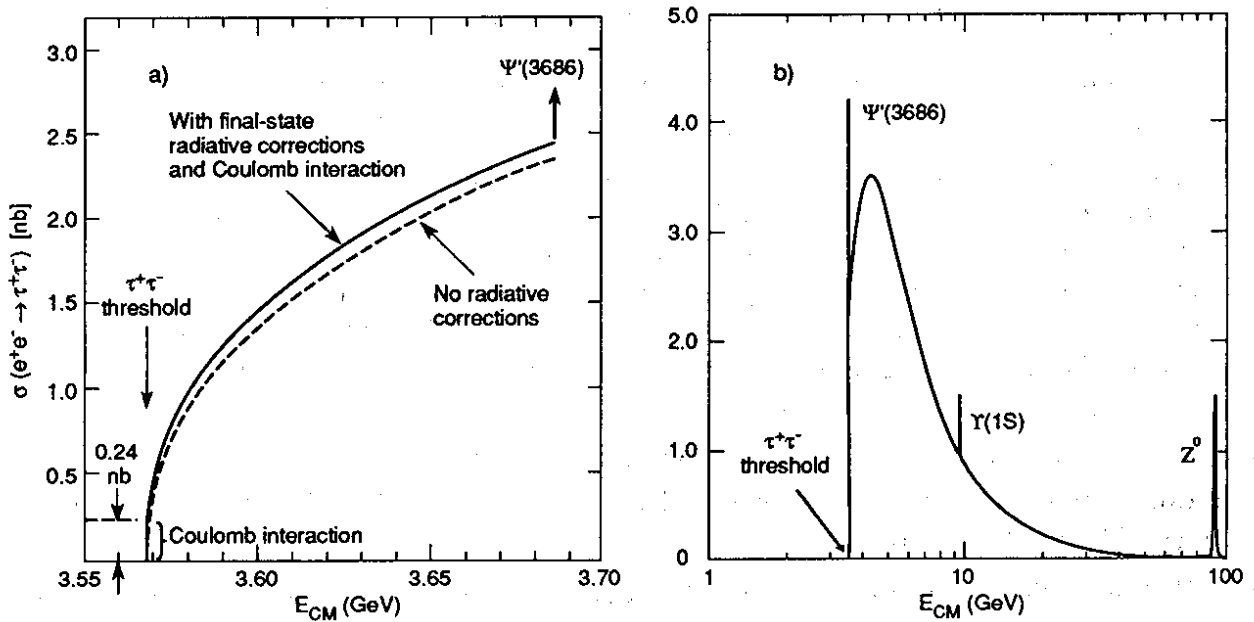


Figure 3: The cross section $\sigma(e^+e^- \rightarrow \tau^+\tau^-)$: a) near threshold[11] (the effects of initial-state radiation are not included); and b) from threshold to 100 GeV.

Particle	Z^0 Factory	B Factory	τ -charm Factory
D^0 (single)	1.2×10^7	1.5×10^7	5.8×10^7 (ψ'')
D^+ (" τ ")	0.5×10^7	0.7×10^7	4.2×10^7 (ψ'')
D_s^+ (" τ ")	0.3×10^7	0.3×10^7	1.8×10^7 (4.14 GeV)
$\tau^+\tau^-$ (pairs)	0.3×10^7	0.9×10^7	0.5×10^7 (3.57 GeV)
			2.4×10^7 (3.67 GeV)
			3.5×10^7 (4.25 GeV)
J/ψ	—	—	1.7×10^{10}
ψ'	—	—	0.4×10^{10}

Table 1: Comparison of the τ and charm yearly samples at several future e^+e^- colliders. The assumed integrated luminosities are 2 fb^{-1} ($L_{peak} = 2 \times 10^{32} \text{ cm}^{-2}\text{sec}^{-1}$; $6.2 \times 10^7 Z^0$'s) at the Z^0 Factory, and 10 fb^{-1} ($L_{peak} = 10^{33} \text{ cm}^{-2}\text{sec}^{-1}$) at B or τ -charm Factories.

- **3.57 GeV.** The $\tau^+\tau^-$ cross-section has a finite value (0.24 nb, ignoring initial-state radiation) precisely at threshold, due to a Coulomb interaction between the τ^+ and τ^- [11]. When the beam energy is set to $m_\tau + \sigma(E)$ (the collision energy spread, which is about 1.0 MeV at this energy) the $\tau^+\tau^-$ cross-section is 0.47 nb, and $\bar{\beta}_\tau = 0.033$. At this energy, the two-body τ decays, such as $\pi^-\nu_\tau$ and $K^-\nu_\tau$, give rise to monochromatic secondaries (see Fig. 6a). The consequences are clean signatures for event selection, as well as *kinematic* separation of the different decay modes. In fact, a monochromator scheme at the interaction point is under study[12, 13, 14] that would reduce the spread in collision energy to about 0.1 MeV. This would allow the τ velocity to be further reduced ($\bar{\beta}_\tau \simeq 0.01$), giving rise to sharper monochromatic distributions.
- **3.67 GeV.** This energy provides the highest $\tau^+\tau^-$ cross-section below the ψ' (3.69) and $D\bar{D}$ threshold (3.73 GeV), a region where τ decay is the *only* source of prompt single charged leptons and prompt neutrinos (which have the distinctive experimental signature of “missing energy”, E_{miss}).
- ψ' (**3.69**). The ψ' constitutes another important channel for clean QCD studies, as well as another high-rate source for calibration of the detector. Furthermore, the highest $\tau^+\tau^-$ cross-section occurs at this energy, and experiments that are free of backgrounds—such as neutrino-less rare τ decays—could be made here. The observed $\tau^+\tau^-$ cross-section at the ψ' is approximately proportional to $1/\sigma(E)$. The $\tau^+\tau^-$ cross-section at the ψ' in Fig. 3b) corresponds to the standard optics; the monochromator scheme would raise the cross-section to $\simeq 10$ nb.
- ψ'' (**3.77**). This energy provides pure $D^0\bar{D}^0$ and D^+D^- final states, without contamination from other charmed particles or from jet fragments, thereby allowing studies of *tagged* D^0 and D^\pm decays.
- **4.03 GeV.** This energy provides the highest charm cross section in e^+e^- annihilation and is suitable for tagged D_s^\pm studies.
- **4.14 GeV.** This is a second identified energy for D_s^\pm studies, via $D_s^\pm D_s^{*\mp}$ events. In fact there may be better operating points for D_s^\pm studies, since present measurements of the hadronic cross section and charmed particle yields in this region are poor. If this

remains the case, an early part of the τ CF physics programme would be a precise scan of the hadronic and charm cross sections over the entire threshold region.

2.2 Backgrounds

A key experimental feature of the τ -charm Factory is the ability to measure backgrounds experimentally, by lowering the beam energy below threshold. This can be done for τ data samples (backgrounds are measured at 3.56 GeV), for D^0/D^\pm data samples (backgrounds are measured below the $\psi''(3.77)$) and for D_s^\pm data samples (backgrounds are measured below 3.94 GeV). Furthermore, the charm data are free of heavier-flavour (b quark) backgrounds and free of jet fragments, both of which are present at higher energies. As for the τ data, they are entirely free of heavy quark (b and c) backgrounds—a feature that is unique to the threshold region.

Another important experimental feature of the τ -charm threshold region is the ability to tag a particle under study. The $D\bar{D}$ or $\tau\bar{\tau}$ event can be cleanly isolated by identifying the decay of only one of the particles, thereby “single-tagging” (identifying) the other particle without imposing any requirements on its type of decay. Single-tagging has important advantages: reduced biases, presence of kinematic constraints, exact flux normalization and, near to threshold, extremely low backgrounds. This technique has been used extensively at the $\psi''(3.77)$, e.g. to provide unique measurements of D^0 and D^\pm absolute branching ratios. In the case of D_s^\pm , however, absolute branching ratio measurements have not yet been possible since the statistics are too poor; in fact not a single example exists of a double-tagged $D_s^+D_s^-$ event (in which both particles in the event are independently identified). The τ -charm Factory can collect huge single-tagged samples: 7×10^6 D^0 's ($\psi''(3.77)$), 4×10^6 D^\pm 's ($\psi''(3.77)$), and 10^6 D_s^\pm 's (4.14 GeV) per year, at the indicated energies. At other machines, only D^0 's can be tagged via the soft π^+ in $D^{*+} \rightarrow D^0 \pi^+$, albeit with substantially higher backgrounds than the $D^0\bar{D}^0$ tag at the $\psi''(3.77)$.

Furthermore, at a τ -charm Factory it will be possible—for the first time at any machine—to single-tag $\tau^+\tau^-$ events. Previous measurements have employed global selection criteria which have restricted *both* τ decays. Single-tagging requires a clean signature from a single τ decay. With the capability of the τ -charm Factory to produce $\tau^+\tau^-$ copiously near threshold, uncontaminated by heavy flavours, there are several distinct signatures: $e+E_{miss}$, $\mu+E_{miss}$, and monochromatic- $\pi+E_{miss}$ (at 3.57 GeV). The missing energy is measured in a hermetic detector. Hermeticity is provided by precise magnetic analysis, a crystal electromagnetic calorimeter, and a fine-grained hadron calorimeter that detects K_L^0 's and n 's. Studies[15, 16] indicate backgrounds of between 10^{-3} (at 3.57 GeV) and 10^{-4} (at 3.67 GeV) in the case of the $e+E_{miss}$ trigger, which has a $\tau^+\tau^-$ event detection efficiency of 24%.

For comparison, the typical background contaminations in present samples of *double*-tagged $\tau^+\tau^-$ events at B or Z^0 Factory energies are about 5%[6]. The lowest backgrounds achieved in LEP data are about 1%, while retaining adequate detection efficiency. This corresponds to a $q\bar{q}$ rejection of $\simeq 4 \times 10^{-4}$, to be compared with $\simeq 10^{-5}$ for single-tagging at the τ -charm Factory.

2.3 Systematic errors

The excellent suppression of backgrounds—and the ability to measure them experimentally—should result in small systematic errors due to background uncertainties.

Systematic effects in single-tagged events are minimized since *all* the remaining particles come from a single, identified parent and no restrictions are imposed on its decay topology. Single-tagging also allows precise measurement of branching ratios, since there is zero normalization uncertainty; elsewhere, branching ratio measurements rely on estimations of the τ or D cross-sections and measurements of the luminosity.

Systematic errors arising from uncertainties in the detector performance can also be carefully monitored at the τ -charm Factory. The design momentum measurement accuracy

$$[\sigma_p/p]^2 = [0.3\%p(\text{GeV}/c)]^2 + [0.3\%/\beta]^2$$

results in a mass resolution of 2 MeV/c² at the $\tau \rightarrow \nu_\tau 5\pi^\pm$ end-point, where the ν_τ mass will be measured (Section 3.1.1). However, in order to benefit from such precision, it is necessary to maintain the absolute momentum-scale error below 0.1% (which is equivalent to a 2 MeV/c² mass shift). This figure is at the limit of what has been achieved so far by a collider detector. Precise systematic control of the momentum scale of the τ cF detector will be achieved by periodically recording data at $\psi''(3.77)$ and reconstructing background-free $D^\pm \rightarrow 5 - \text{prong}$ events. These events correspond closely to the mass region at the $\tau \rightarrow \nu_\tau 5\pi^\pm$ end-point. In addition, there will be frequent, high-statistics calibrations of all the detector responses and resolutions at the J/ψ and ψ' . With these calibration signals, it should be possible to maintain the momentum-scale error of the τ -charm Factory detector below 0.1%.

In addition to excellent momentum measurements, there are advantages for photon detection and particle identification near τ -charm threshold. Since particles are produced isotropically, the detection inefficiency caused by charged and neutral pileup is minimized. This is especially important in the case of τ decays involving several neutral particles (Fig. 4), which seem to be associated with the “one-prong problem” (Section 3.1.2). A further advantage is that the kinematic limit of particles from τ or D decays at rest is $\simeq 1$ GeV/c and so the identification of π , K and p is easier than at higher energy machines.

3 Physics highlights

In this section, we give an overview of the physics programme of the τ -charm Factory. Only a few topics have been selected from the exceptionally-broad range that will be studied at the τ -charm Factory. Many of the results presented here come from the extensive studies on τ -charm physics that have been made in workshops at SLAC[5], Orsay[6], Sevilla[7] and CERN[8].

3.1 Tau physics

3.1.1 ν_τ MASS

There is no fundamental principle in the Standard Model that requires exactly massless neutrinos, and many extensions of it include finite masses. Finite neutrino masses would

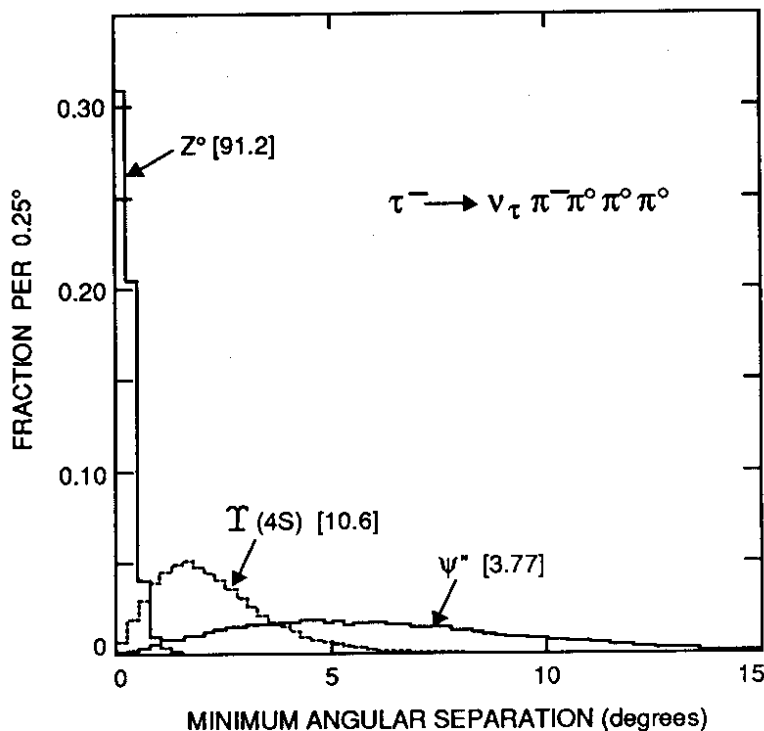


Figure 4: The minimum angular separation between any two particles (charged and/or neutral) in $e^+e^- \rightarrow \tau^+\tau^-$, where $\tau^+ \rightarrow e^+\nu_e\bar{\nu}_\tau$ and $\tau^- \rightarrow \pi^- 3\pi^0 \nu_\tau$ [17]. For comparison, an excellent 2γ resolution is $\simeq 1^\circ$ (ALEPH).

profoundly affect the Standard Model—allowing mixing and oscillations between lepton families—and also provide answers to two of the major puzzles of cosmological physics: the deficiency of solar neutrinos and the composition of the dark matter of the Universe.

Many models of new physics predict a mass hierarchy between the three generations of neutrinos, as is observed for the charged leptons. For example, in the “see-saw” model[18], $m_{\nu_i} \propto m_i^2$, in which case a sensitivity of $1 \text{ MeV}/c^2$ for m_{ν_τ} is equivalent to $0.1 \text{ eV}/c^2$ for m_{ν_e} . Within such models, therefore, an experimental sensitivity of $\mathcal{O}(1 \text{ MeV}/c^2)$ for m_{ν_τ} is more sensitive to new physics than the best mass limits that can be obtained for m_{ν_μ} and m_{ν_e} .

A ν_τ in the mass range 1 to 20 MeV/c^2 is expected to affect substantially the successful predictions for the primordial nucleosynthesis of light isotopes in the early Universe. It has been proposed[19] that this cosmological argument could exclude this mass region, provided the ν_τ lifetime is greater than 1 sec. The few- MeV/c^2 region for m_{ν_τ} appears in left-right symmetric or related models with a L-R symmetry breaking scale $\simeq 10^4 - 10^5 \text{ GeV}$ (using the see-saw mechanism). This region of ν_τ -masses ($\simeq 1\text{-}35 \text{ MeV}/c^2$) has also been suggested in trying to explain the baryon-antibaryon asymmetry of the Universe[20], or to make the ν_τ an acceptable candidate for cold dark matter[21].

The ν_τ mass is investigated by measuring the end-point of the $5\pi^\pm$ mass spectrum in $\tau^\pm \rightarrow 5\pi^\pm \nu_\tau$, and the end-point of the $K^-K^+\pi^\pm$ mass spectrum in $\tau^\pm \rightarrow K^-K^+\pi^\pm \nu_\tau$. With a two-year (20 fb^{-1}) sample at 3.67 GeV, the statistical upper limits (95% CL) on the ν_τ mass are $3.5 \text{ MeV}/c^2$ from $\tau^\pm \rightarrow 5\pi^\pm \nu_\tau$ events (Fig. 5)[22, 23], and $10 \text{ MeV}/c^2$ from $\tau^\pm \rightarrow K^-K^+\pi^\pm \nu_\tau$ events[24]. Combining both decays gives an upper limit (95% CL) of 3.3

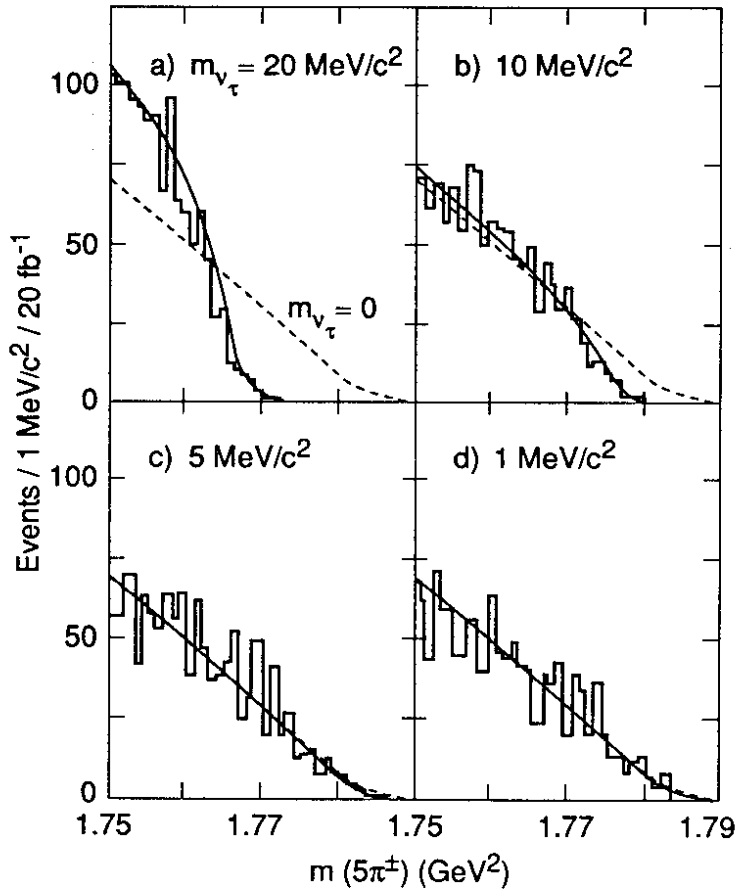


Figure 5: The endpoint spectra for the $5\pi^\pm$ invariant mass in the decay $\tau^\pm \rightarrow 5\pi^\pm \nu_\tau$. Several values of m_{ν_τ} are assumed, as indicated. The distributions come from a Monte Carlo data sample equivalent to two years (20 fb^{-1}) at 3.67 GeV [22].

MeV/c^2 , to be compared with the present limit of $35 \text{ MeV}/c^2$ [25]. In order to realize this accuracy, very careful control of backgrounds and systematic errors will be required.

The τ -charm Factory is also indirectly sensitive to ν_τ masses below $\mathcal{O}(1 \text{ MeV}/c^2)$, as discussed in Section 3.1.4.

To reach a direct limit of $\mathcal{O}(1 \text{ MeV}/c^2)$ on m_{ν_τ} , the present m_τ error of $3\text{-}4 \text{ MeV}/c^2$ [26] must be reduced. This can only be done near threshold, by measuring $\sigma(e^+e^- \rightarrow \tau^+\tau^-)$. The expected precision at BEPC or the τ -charm Factory is $\simeq 0.1 \text{ MeV}/c^2$. This will require an absolute calibration of the beam energy to an accuracy of $\mathcal{O}(10^{-5})$ using the resonance depolarization technique developed at Novosibirsk[27]. An accurate value of the τ mass is also needed to test lepton-universality through the comparison of the τ -lifetime and its leptonic branching ratios.

3.1.2 PRECISE BRANCHING RATIOS

Many of the decay modes of the τ lepton are precisely described in the Standard Model, including the decay rates and the angular and helicity distributions of final-state particles[28, 29, 9]. Each of these predictions can be used to test for the presence of new interactions

Ratio	No electroweak corrections	With electroweak corrections	Experimental value
$\mu^- \bar{\nu}_\mu \nu_\tau / e^- \bar{\nu}_e \nu_\tau$	0.973	0.973	1.01 ± 0.03
$\pi^- \nu_\tau / e^- \bar{\nu}_e \nu_\tau$	0.607	0.601	0.62 ± 0.03
$K^- \nu_\tau / e^- \bar{\nu}_e \nu_\tau$	0.0395	0.0399	0.038 ± 0.011

Table 2: Standard Model predictions[33] and experimental values for $\tau \rightarrow 1\text{-prong} + 0\gamma$ relative branching ratios.

	$e^- \bar{\nu}_e \nu_\tau$	$\mu^- \bar{\nu}_\mu \nu_\tau$	$\pi^- \nu_\tau$	$K^- \nu_\tau$
Present experiments	2.3%	2.3%	4.5%	28.%
τ -charm Factory	0.15%	0.15%	0.2%	0.8%

Table 3: Experimental precisions of $\tau \rightarrow 1\text{-prong} + 0\gamma$ branching ratios.

beyond the Standard Model.

The τ -charm Factory will carry out a precise, systematic search among all τ decay channels for signs of discrepancies with the theoretical expectations. In certain cases, improved experimental measurements will be required elsewhere in order to sharpen the theoretical predictions. For example, in the case of vector-current hadronic decays like $\tau^- \rightarrow (4\pi)^- \nu_\tau$, improved measurements are required for the $2\pi^- 2\pi^+$ and $\pi^- \pi^+ 2\pi^0$ cross-sections in $e^+ e^-$ annihilation in the centre-of-mass energy region between 1 and 1.8 GeV. These hadronic cross-sections—which are also needed for calculations of radiative corrections at the Z^0 —should be accurately measured in future at both ϕ - and τ -charm Factories.

Of particular interest is the discrepancy[29] between the inclusive $\tau \rightarrow 1\text{-prong}$ branching ratio (0.861 ± 0.003) and the sum of the exclusive 1-prong decays ($\leq .802 \pm 0.014$)—the so-called “one-prong problem”. It is difficult to study the origin of the one-prong deficit because the experimental discrepancy is just at the limit of the statistical and systematic errors of a single experiment, and some caution has to be applied when combining results from different experiments. With the results of the more-recent high statistics measurements, the one-prong deficit has been reduced but the situation is still quite confusing: while CELLO[30] and ALEPH[31] find that the sum of the measured exclusive modes, $(100.4 \pm 1.8)\%$ [31], saturates the inclusive width, ARGUS[32] finds that the sum of the exclusive modes, $(91.0 \pm 1.4 \pm 3.0)\%$, leaves a significant fraction of the total τ -width unaccounted for.

The decay modes $e^- \bar{\nu}_e \nu_\tau$, $\mu^- \bar{\nu}_\mu \nu_\tau$, $\pi^- \nu_\tau$ and $K^- \nu_\tau$ are theoretically understood (Table 2) [33] at the level of the electroweak radiative corrections (1%). New physics could affect these branching ratios as perhaps a non-standard Cabibbo angle in the τ sector or as a Higgs field. For example, it is possible that the leptons may get their masses from a Higgs field that is separate from that of the quarks[11]. This Higgs would couple exclusively to leptons and proportionally to the lepton mass. Evidently, τ decays provide the best environment to study such a Higgs boson. The effects of a charged Higgs could be seen elsewhere in τ decays, such as the angular distributions in $\tau^- \rightarrow \pi^- \pi^0 \nu_\tau$ [34].

In the τ -charm Factory, the expected precisions on the 1-prong branching ratios are 0.1% (e, μ, π) - 0.8% (K) [22] in a one-year data sample, whereas present errors are 2% - 30% (Table 3). These precise measurements would allow a test of the universality of the leptonic

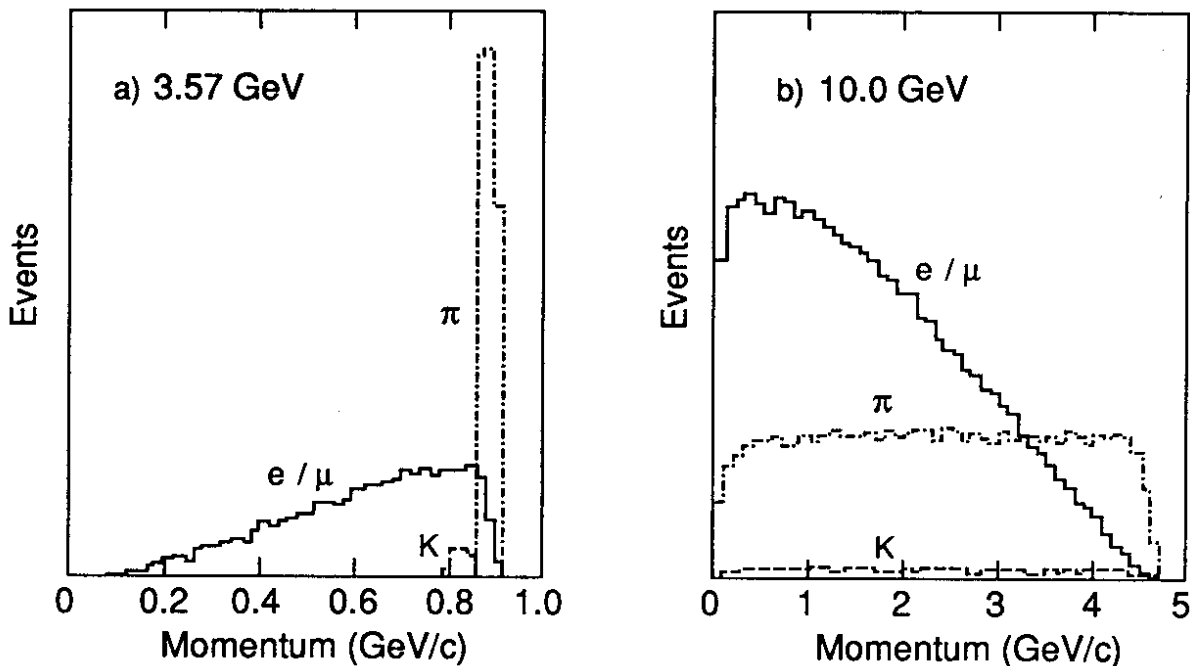


Figure 6: The momentum spectra from single-charged-particle τ decays at centre-of-mass energies of a) 3.57 GeV (2 MeV above $\tau^+\tau^-$ threshold) and b) 10 GeV.

charged-currents at the 0.1% level, to be compared with the present accuracies of 0.6% for g_μ/g_e and 2% for g_τ/g_μ [9]. The test on the τ -coupling requires an accurate value of the τ -lifetime, which can be obtained at LEP. For comparison, LEP will probably get an accuracy of about 0.8% in the $e^-\bar{\nu}_e\nu_\tau$ and $\mu^-\bar{\nu}_\mu\nu_\tau$ branching ratios, while a precision of only about 1.5% seems to be possible for the sum of the $\pi^-\nu_\tau$ and $K^-\nu_\tau$ modes.

The experimental requirements to achieve precise— $\mathcal{O}(0.1\%)$ —measurements of the τ branching ratios are very challenging; the normalization, detection efficiency and backgrounds must each be known at the 0.1% level. These requirements can probably be achieved only at the τ -charm Factory, running just above $\tau^+\tau^-$ threshold at 3.57 GeV, where the decays are kinematically-separated (Fig. 6a). In contrast, at higher energies the distributions completely overlap (e.g. Fig 6b) and the particle identification requirements—especially between π and K —are more severe. At the τ -charm Factory, the backgrounds from all non- τ sources, which are calculated to be of $\mathcal{O}(0.1\%)$, will be experimentally measured by reducing the beam energy by 10 MeV and recording data below $\tau^+\tau^-$ threshold.

3.1.3 CURRENT STRUCTURE OF THE $\tau\nu_\tau W$ VERTEX

High-precision μ experiments have showed that the interaction mediating μ decay is indeed of the predicted V-A nature[35]. The form of the $\tau\nu_\tau W$ vertex, although consistent with the Standard Model, is poorly known in comparison. The τ -charm Factory would make a comprehensive study of the leptonic τ -decay modes, constraining the underlying dynamics with a precision comparable to, or even better than, that of the μ .

The experiment involves a precise determination of the decay parameters— $\rho_l, \eta_l, \xi_l, \delta_l$ ($l = e, \mu$), and ξ'_μ —in the leptonic channels $\tau^- \rightarrow e^-\bar{\nu}_e\nu_\tau$ and $\tau^- \rightarrow \mu^-\bar{\nu}_\mu\nu_\tau$. The Michel

and low-energy spectral shape parameters, ρ and η , respectively, are determined by the e, μ energy distributions. The asymmetry parameters ξ and δ —which describe the asymmetry of the daughter lepton (e or μ) relative to the τ spin—are determined from angular correlations between, for example, $\tau^- \rightarrow e^- \bar{\nu}_e \nu_\tau$ and $\tau^+ \rightarrow \pi^+ \bar{\nu}_\tau$. Finally, the polarization parameter ξ'_μ can be determined from a measurement of the μ polarization with a μ polarimeter. In the Standard Model, $\rho = \delta = 3/4$, $\eta = 0$ and $\xi = \xi' = 1$. These parameters are sensitive to novel objects such as a charged Higgs or a right-handed boson (in fact, the μ -decay analogue provides the best limits on right-handed currents).

The experimental approach has been evaluated in detail by Fetscher[36] in the e^+e^- energy range from $\tau^+\tau^-$ threshold up to 20 GeV. He finds relatively small (factor 2) differences in the *statistical* sensitivity to the decay parameters over this range: ξ and δ favour the higher energies and ρ, η and ξ'_μ favour threshold.

However, high precision measurements of these parameters are likely to be dominated by systematic uncertainties. As an example, the Crystal Ball has measured the Michel parameter at $E_{\text{cm}} \simeq 10$ GeV to be $\rho = 0.64 \pm 0.06(\text{stat.}) \pm 0.07(\text{syst.})$ [37]. An important contribution to the systematic error was due to the large radiative correction ($\Delta(\rho) = -0.20$). At threshold, however, the experimental data require small radiative corrections since the τ 's are almost at rest and radiation can only bring them closer to rest. Additional advantages of the threshold region are the low backgrounds and better separation of the individual 1-prong decays. Backgrounds may in fact preclude the measurement of η at higher energies. The expected accuracies are 0.3% for ρ ; 1% for η, ξ and δ ; and 10% for ξ'_μ [22]. With this precision it will be possible to search for signs of a right-handed coupling up to $m_{W_R} \simeq 500$ GeV/ c^2 . So far, only ρ has been measured, to 4% accuracy[38].

3.1.4 RARE AND FORBIDDEN DECAYS

The Standard Model predicts several rare decays of the τ , such as $\tau^- \rightarrow \pi^- \eta \nu_\tau$, and also it forbids decays that involve lepton number violation, such as $\tau^- \rightarrow l^- \gamma, l^- \mu^+ \mu^-, l^- e^+ e^-, h^0 l^-, h^- e^- \mu^+$ etc., with $l=e, \mu$ and $h = \text{hadron}(s)$ [16, 39, 40]. Forbidden decays could be induced by any one of a broad range of new processes, such as Higgs, SUSY, leptoquarks, technicolour and compositeness. Since the τ is a third generation lepton, new physics associated with Higgs couplings is expected to give larger effects than for the lighter leptons. The higher mass of the τ also means that many more decays are kinematically-allowed, thereby broadening the search for surprises.

The observed separate conservation of baryon number B and lepton numbers L_e, L_μ and L_τ is specific to the minimal Standard Model, and many of its extensions violate these symmetries. In particular, several supersymmetric models lead to lepton-number violating rates which may be constrained at the τ -charm Factory[41, 42, 43]. For example, $\tau^- \rightarrow \mu^- \gamma$ may occur with a branching ratio in the range $10^{-8} - 10^{-4}$. This type of process also appears in models (supersymmetric or not) with extra heavy vector-like fermions[44].

The decay $\tau^- \rightarrow \pi^- \eta \nu_\tau$ can only occur through second-class weak currents (which have never been observed) or through non-standard mechanisms such as the violation of G parity or the existence of a new scalar particle. The branching ratio expected in the Standard Model due to the violation of G parity (from the $u - d$ quark mass difference) is about 10^{-5} [45]. A Monte Carlo study shows that this decay can be cleanly measured at 3.67 GeV[46].

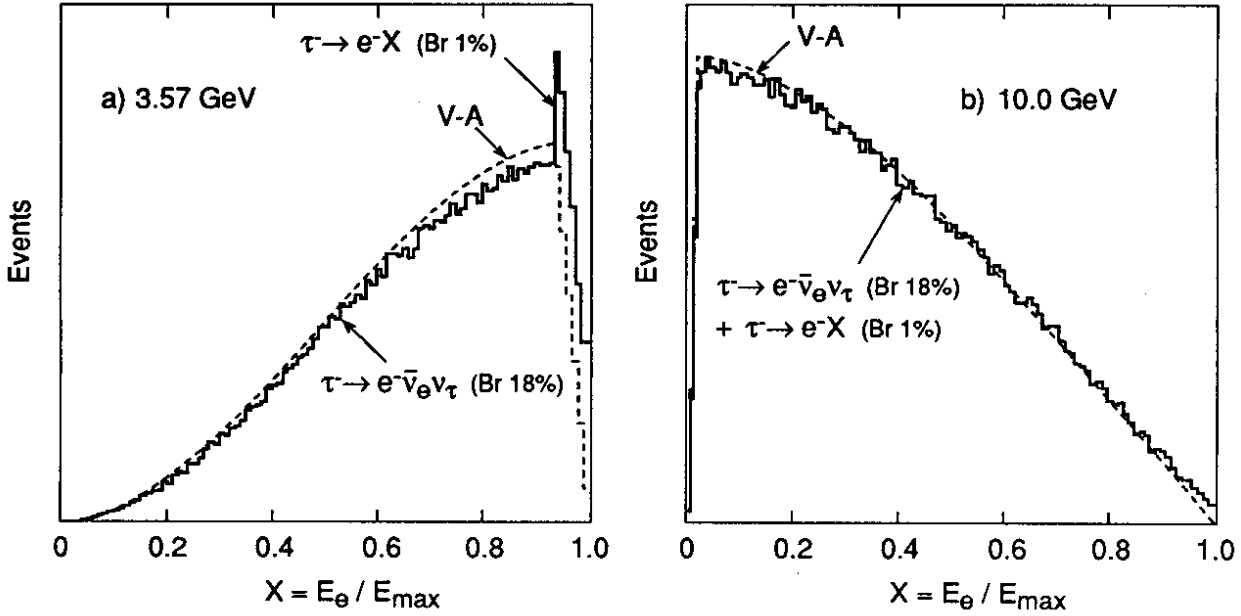


Figure 7: The combined electron spectra (solid histograms) from the standard decay $\tau^- \rightarrow e^- \bar{\nu}_e \nu_\tau$ (Br 18%) together with a hypothetical two-body decay $\tau^- \rightarrow e^- X$ (Br 1%) at centre-of-mass energies of a) 3.57 GeV and b) 10 GeV [52]. The particle X is a massless Goldstone boson. The dashed histograms show conventional (V-A) fits to the combined spectra. Each plot contains 200 k $\tau^- \rightarrow e^- \bar{\nu}_e \nu_\tau$ events (corresponding to two month's data at 3.57 GeV).

The optimum energy to search for forbidden τ decays is also at 3.67 GeV, where a simple and ($\simeq 100\%$) efficient tag, $E_{miss} \geq 0.8$ GeV, can be used. The validity of any signal can be convincingly demonstrated by its disappearance at 3.56 GeV. The τ -charm Factory will be able to place upper limits of $\text{Br} \simeq 10^{-8}$ on these decays, or observe them at a higher value. These limits would probe mass scales up to $\simeq 4$ TeV, for a conservative electroweak coupling strength. If the monochromator optics is successful, it may be possible to reach even higher sensitivities for certain rare τ decays at the $\psi'(3.69)$. Here the production rate is at a maximum (Section 2.1) and the backgrounds for neutrinoless (fully-reconstructed) τ decays are small.

The particular case $\tau^- \rightarrow 3l^\pm$ ($l = e, \mu$) would be induced by a lepton flavour violating coupling of the Z^0 boson, $Z^0 \rightarrow l^\pm \tau^\mp$. The τ -charm Factory should reach the upper limit $\text{Br}(\tau^- \rightarrow 3l^\pm) < 2 \times 10^{-8}$, which is equivalent to $\text{Br}(Z^0 \rightarrow l^\pm \tau^\mp) < 10^{-7}$ [47] and probably beyond the sensitivity of HLEP.

Rare decays of the τ will also provide the τ -charm Factory with a sensitivity to finite-mass ν_τ 's below the direct measurement limit[48, 49]. For example, if the 17 keV neutrino reported by Simpson and others[50] is indeed a heavy ν_τ admixed with ν_e , then it would have to decay in order to agree with the observed density of the Universe. In fact, by the same argument, *any* ν_τ heavier than $\mathcal{O}(100 \text{ eV}/c^2)$ would have to decay. The decays

$$\nu_\tau \rightarrow \nu_l X \quad (l = e, \mu)$$

are then expected, where X is a massless, weakly interacting, spin zero Goldstone boson

(Majoron, familon, flavon, etc.). The τ lepton would then also be able to decay through same process

$$\tau^- \rightarrow l^- X$$

and the expected branching ratios are in the range $10^{-6} - 10^{-2}$ [49, 51].

The τ -charm Factory is uniquely-suited to search for these rare τ decays, which lead to the distinctive signature of monochromatic leptons (Fig. 7a)[52]. In contrast, the sensitivity is much weaker at higher energies since the lepton spectrum from the $l^- X$ decay is broad, spreading over the full spectrum of the standard $l^- \bar{\nu}_l \nu_\tau$ decay (Fig. 7b). The expected branching-ratio sensitivity at the τ -charm Factory is better than 10^{-5} , to be compared with the present limits of 1-2%. The experimental sensitivity could be improved a further order-of-magnitude if the monochromator optics is successful (Section 2.1). Sensitivity to still-lower branching ratios would require improvements in the πe rejection of the τ CF detector, e.g. with a fast RICH.

3.1.5 CP VIOLATION IN THE LEPTON SECTOR

Non-zero electric dipole moments of leptons, d_l , are unambiguous signals of T (CP) violation, and are sensitive probes of physics beyond the Standard Model. The electric dipole moments are expected to be small in the Standard Model, well below the present experimental bounds. New physics can lead to much larger effects, e.g. Higgs models indicate $|d_\tau| \simeq 10^{-22} e$ [53]. Given the present lack of understanding of CP violation, any experimental data—even bounds—are valuable.

The precise measurement of the $\tau^+ \tau^-$ production cross-section at the τ -charm Factory (expected accuracy $\simeq 0.1$ -0.3 %) could improve the present bound on the τ electric dipole moment ($|d_\tau| < 6 \times 10^{-16} e \text{ cm}$ [54]; $|d_\tau(30\text{GeV})| < 1.4 \times 10^{-16} e \text{ cm}$ [55]) by more than one order of magnitude[9]. The same is true for the measurement of the (CP-conserving) anomalous τ magnetic moment, which is poorly tested at present ($|a_\tau(\text{LEP})| < 0.11$; $|a_\tau(30\text{GeV})| < 0.01$)[9]. An intrinsic T-odd test can be done by studying T-odd triple correlations of the final τ -decay products in the processes $e^+ e^- \rightarrow \tau^+ \tau^- \rightarrow (X_1^- \nu_\tau)(X_2^+ \bar{\nu}_\tau)$. The estimated sensitivity at the τ -charm Factory is $|d_\tau| \leq 10^{-17} e \text{ cm}$ [56]. For comparison, the current bounds on the lighter leptons are $d_e = (-2 \pm 6) \times 10^{-26} e \text{ cm}$ and $d_\mu = (3.7 \pm 3.4) \times 10^{-19} e \text{ cm}$.

3.1.6 QCD

The τ is the only known lepton that is massive enough to decay into hadrons. Its semileptonic decays are therefore a unique laboratory for studying the hadronic weak currents in very clean conditions. In addition to providing valuable information on the vector current, which would complement the measurements of $e^+ e^- \rightarrow \gamma \rightarrow \text{hadrons}$, hadronic τ -decay modes are the only available tool to perform an accurate study of the axial-vector spectral functions. The clean, high-statistics data samples of the τ -charm Factory would be very useful in understanding the couplings of the low-lying mesons to the weak currents, and would allow many interesting tests of QCD to be made[57].

3.2 Charm physics

3.2.1 $D^0\bar{D}^0$ MIXING AND CP VIOLATION

The rate for $D^0\bar{D}^0$ oscillations is expected[58] to be quite small in the Standard Model,

$$r_D \equiv \frac{\text{Br}(D^0 \rightarrow \bar{D}^0 \rightarrow \bar{f})}{\text{Br}(D^0 \rightarrow f)} \leq 10^{-5} - 10^{-4}.$$

The reasons for such a suppression are very specific to the structure of the Standard Model and so many of its extensions (SUSY models, vector-like fermions, E6-like models, etc.) lead to enhanced transition amplitudes.

Signatures of mixing are like-sign dileptons from dual semileptonic decays ($l^\pm l^\pm X$) or dual identical hadronic decays, such as $(K^+\pi^-)(K^+\pi^-)$ or $(K^-\pi^+)(K^-\pi^+)$. At the τ -charm Factory, the latter can be separated from doubly Cabibbo-suppressed decays since quantum statistics yield different correlations in the $D\bar{D}$ decays from $D^0\bar{D}^0$, $D^0\bar{D}^0\gamma$, and $D^0\bar{D}^0\pi^0$ [58, 59]. The τ -charm Factory can observe mixing at the limit $r_D \approx 2 \times 10^{-5}$ with one year's data[60, 10], to be compared with the present 90% C.L. limit, $r_D < 3.7 \times 10^{-3}$.

A rate difference between $D^0\bar{D}^0 \rightarrow (l^+X)(f)$ and $\bar{D}^0D^0 \rightarrow (l^-X)(f)$, with f a CP eigenstate (e.g. K^+K^-) would provide an unambiguous signal of CP violation, either direct or involving $D^0\bar{D}^0$ mixing. A CP asymmetry of about 1% could be measured[60] in a one-year sample of $D^0\bar{D}^0\gamma$ events at $E_{cm} = 4.14$ GeV. The sensitivity to direct CP violation in the decay amplitude is similar in the process $\psi''(3.77) \rightarrow D^0\bar{D}^0 \rightarrow f(D^0)f(\bar{D}^0)$, with f 's of the same CP parity, such as $f = K^+K^-$. A single event of this type would establish CP violation, since the initial state is CP-even whereas the final state (p wave) is CP-odd. Although these sensitivities are expected to be insufficient to observe an effect, according to the Standard Model, the τ -charm Factory would nevertheless provide an important first window on CP violation in the up-quark sector.

3.2.2 THE CKM MATRIX ELEMENTS V_{cs} AND V_{cd}

Although constrained by Standard Model unitarity to 0.1% (V_{cs}) and 1% (V_{cd}), the CKM charm matrix elements are poorly measured at present ($\pm 10-20\%$). At the τ -charm Factory the D semileptonic branching ratios could be measured with an accuracy better than 1% [61, 62], whereas present errors are 12% for $D^0 \rightarrow K^-e^+\nu_e$ and 50% for $D^0 \rightarrow \pi^-e^+\nu_e$. The ability of the τ -charm Factory to measure with high precision all the relevant axial and vector form-factors should provide the necessary information to select among or improve the existing models of D and B meson decays. This would allow better estimates to be made of the form-factors, which are needed to extract the CKM matrix elements. Theoretical uncertainties are largely avoided by taking ratios of branching ratios. In this way, V_{cd}/V_{cs} can be determined to 1%, which is comparable to the present precision of $\theta_{Cabibbo}$.

3.2.3 PURE LEPTONIC D DECAYS

Pure leptonic decays of $D_{(s)}^\pm$ mesons (Fig. 8) can be rigorously calculated in the Standard Model. The predicted branching ratios are

$$\text{Br}(D^+ \rightarrow l^+\nu_l) = \tau_{D^+} \frac{G_F^2}{8\pi} f_D^2 m_D |V_{cd}|^2 \times m_l^2 \left(1 - \frac{m_l^2}{m_D^2}\right)^2 \quad (1)$$

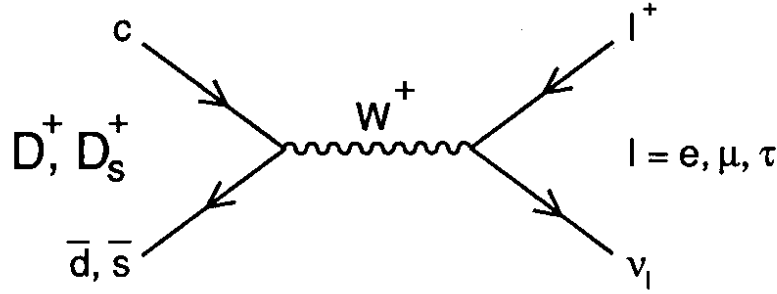


Figure 8: Pure leptonic D^\pm or D_s^\pm decay diagram.

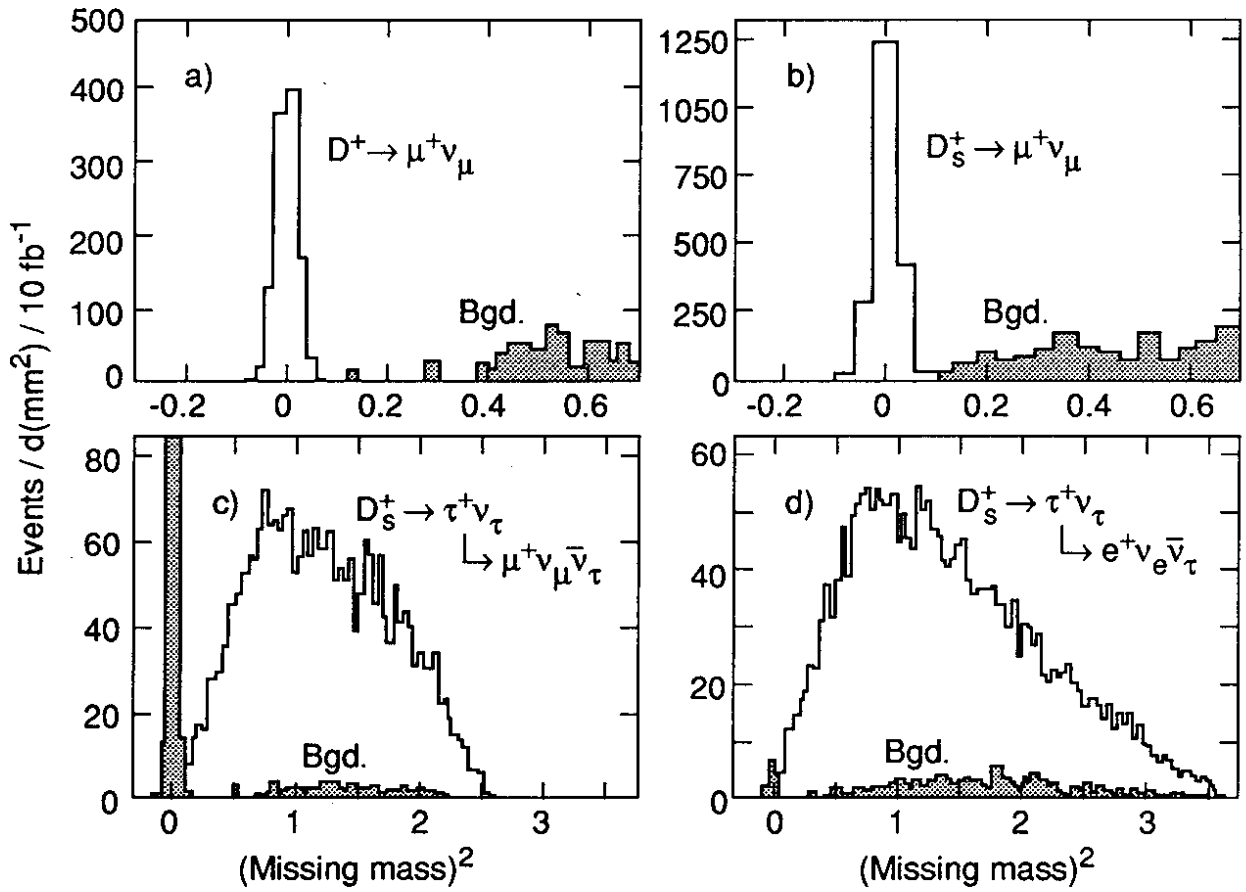


Figure 9: Measurement of pure leptonic D decays in the τ cF detector[63]. Missing masses in single-tagged events are shown for: a) $D^+ \rightarrow \mu^+ \nu_\mu$ ($\simeq 1100$ events per year); b) $D_s^+ \rightarrow \mu^+ \nu_\mu$ ($\simeq 2000$ events per year); c) $D_s^+ \rightarrow \tau^+ \nu_\tau$, $\tau^+ \rightarrow \mu^+ \nu_\mu \bar{\nu}_\tau$ ($\simeq 2000$ events per year); and, d) $D_s^+ \rightarrow \tau^+ \nu_\tau$, $\tau^+ \rightarrow e^+ \nu_e \bar{\nu}_\tau$ ($\simeq 2400$ events per year). The indicated statistics correspond to 10 fb^{-1} ($L = 10^{33} \text{ cm}^{-2} \text{ sec}^{-1}$) and $f_D \simeq 200 \text{ MeV}$. The background events are shaded.

$$Br(D_s^+ \rightarrow l^+ \nu_l) = \tau_{D_s^+} \frac{G_F^2}{8\pi} f_{D_s}^2 m_{D_s} |V_{cs}|^2 \times m_l^2 \left(1 - \frac{m_l^2}{m_{D_s}^2}\right)^2. \quad (2)$$

This indicates the largest pure leptonic branching ratios will be $Br(D_s^+ \rightarrow \tau^+ \nu_\tau) \simeq 3.3\%$, $Br(D_s^+ \rightarrow \mu^+ \nu_\mu) \simeq 3.6 \times 10^{-3}$, and $Br(D^+ \rightarrow \mu^+ \nu_\mu) \simeq 3.5 \times 10^{-4}$.

Measurements of the pure leptonic D decays are important in determining the weak decay constants f_D and f_{D_s} (equations (1) and (2)), which measure the overlap of the c and $d(s)$ quarks in the $D_{(s)}^\pm$ mesons. The decay constants appear in the theory of second-order weak processes—including mixing and CP violation—and are therefore important quantities to be experimentally determined. Precise measurements of these constants would also provide important tests of modern methods of calculation in non-perturbative QCD (lattice, sum rules, infinite mass limit), thereby providing a firmer ground for attempts to extrapolate to beauty systems (since f_B is experimentally inaccessible) and allowing a better theoretical description of $D^0 \bar{D}^0$ mixing.

Another important result from measurements of the pure leptonic branching ratios is a precise determination of $|V_{cd}| / |V_{cs}|$ from the ratio

$$\frac{Br(D^+ \rightarrow \mu^+ \nu_\mu)}{Br(D_s^+ \rightarrow \mu^+ \nu_\mu)}$$

since the uncertainty in f_D/f_{D_s} should be small.

Furthermore, the relative value of the D_s^\pm leptonic branching ratios is precisely predicted:

$$\frac{Br(D_s^+ \rightarrow \mu^+ \nu_\mu)}{Br(D_s^+ \rightarrow \tau^+ \nu_\tau)} = \frac{m_\mu^2 [1 - (m_\mu^2/m_{D_s}^2)]^2}{m_\tau^2 [1 - (m_\tau^2/m_{D_s}^2)]^2} = 0.109 \pm 0.003$$

where the error is dominated by the present uncertainty in m_τ . Measurement of the pure leptonic branching ratios would therefore provide a novel test of $\mu - \tau$ universality, involving the process:

$$2^{nd} \text{ family quarks} \xrightarrow{W, X?} \begin{cases} 2^{nd} \text{ family leptons} \\ \text{vs.} \\ 3^{rd} \text{ family leptons} \end{cases}$$

The measurements are sensitive to new physics (X) that does not have the usual helicity suppression of pseudoscalar meson decay or that has mass-dependent couplings. The absence of $e\nu$ final states will provide a further test.

Pure leptonic decays of D mesons require single-tagged event samples and are therefore uniquely accessible at the τ -charm Factory. Tagged event samples are necessary both to suppress backgrounds and to provide a constrained fit for the mass of the missing ν 's (see Fig. 9). A detailed Monte Carlo study[63] indicates that the signals should be clearly distinguished from background processes. With 1-year's data, each of the the branching ratios $Br(D_s^+ \rightarrow \tau^+ \nu_\tau)$, $Br(D_s^+ \rightarrow \mu^+ \nu_\mu)$ and $Br(D^+ \rightarrow \mu^+ \nu_\mu)$ can be measured to about 2% accuracy, which is comparable to the present experimental precision for the ratio $Br(\pi^+ \rightarrow e^+ \nu_e)/Br(\pi^+ \rightarrow \mu^+ \nu_\mu)$.

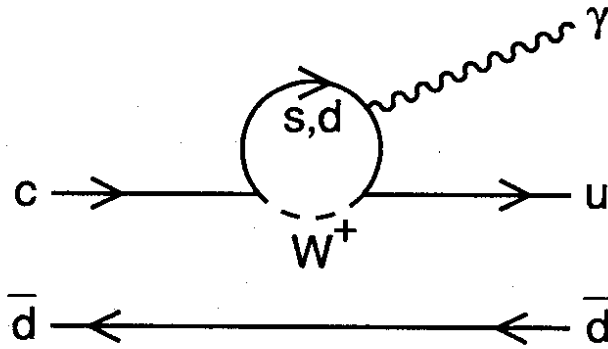


Figure 10: Radiative D decay via a penguin diagram.

3.2.4 RARE D DECAYS

Lepton-flavour-violating decays (such as $D^0 \rightarrow e^\pm \mu^\mp, X e^\pm \mu^\mp$) are completely forbidden for massless ν 's. Flavour changing neutral-current decays (such as $D^0 \rightarrow l^+ l^-, X l^+ l^-, X \nu \bar{\nu}$ and $X \gamma$) may occur in the Standard Model but they are highly suppressed by the GIM mechanism. As an example, radiative penguin processes (Fig. 10) are expected to have branching ratios of $\simeq 10^{-6} - 10^{-5}$ [64]. The τ -charm Factory is probably the only machine that could observe radiative penguin decays of D mesons at the low levels expected. In view of their suppression in the Standard Model, rare D decays are very sensitive to new physics, which may come from contact interactions, leptoquarks, horizontal gauge bosons, substructure, new scalars, technicolour, etc.[65, 40].

Tagging and precise beam-constrained mass measurements suppress backgrounds to these processes. The τ -charm Factory would be sensitive to branching ratios of $\mathcal{O}(10^{-8})$ [66]. Searches for rare decays of D mesons are complementary to those of K or B mesons since the couplings of the new particles may be flavour-dependent, e.g. different for up-like and down-like quarks.

3.3 Charmonium physics

3.3.1 CHARMONIUM AND GLUONIUM SPECTROSCOPIES

The states J/ψ , ψ' and η_c provide a rich field for clean QCD studies[67, 68, 69]. The advantages include the high statistics ($\mathcal{O}(10^{10})$ J/ψ or ψ' events per year), low backgrounds, exclusive decays, and final states with well-defined quantum numbers ($J^{PC} I^G = 1^{-} 0^{-}$).

The τ -charm Factory would make a systematic search for gluonia and hybrids in a gluon-rich environment: $J/\psi \rightarrow \gamma g g, g g g; \eta_c \rightarrow g g$. For example, the decay $J/\psi \rightarrow \gamma g g \rightarrow \gamma X$ involves a pure two-gluon intermediate state with a mass $m_{gg} \leq 3.1$ GeV, i.e. in the expected mass region of the gluonium spectrum. Furthermore, the nature of the state X can be tested experimentally by comparing $J/\psi \rightarrow \gamma X, \omega X$ and ϕX . Resonances that appear in radiative decays but are suppressed with ω and ϕ are likely to be gluonia. The J/ψ is the pre-eminent experimental tool for gluonium spectroscopy and the τ -charm Factory should be able to shed fresh light on the important problem in QCD concerning the dearth of gluonic matter.

The $c\bar{c}$ wave function could be studied via $J/\psi \rightarrow 3\gamma$ and $\eta_c \rightarrow 2\gamma$, which constitute direct tests of the charmonium models. Moreover, the huge amount of η_c and χ events at

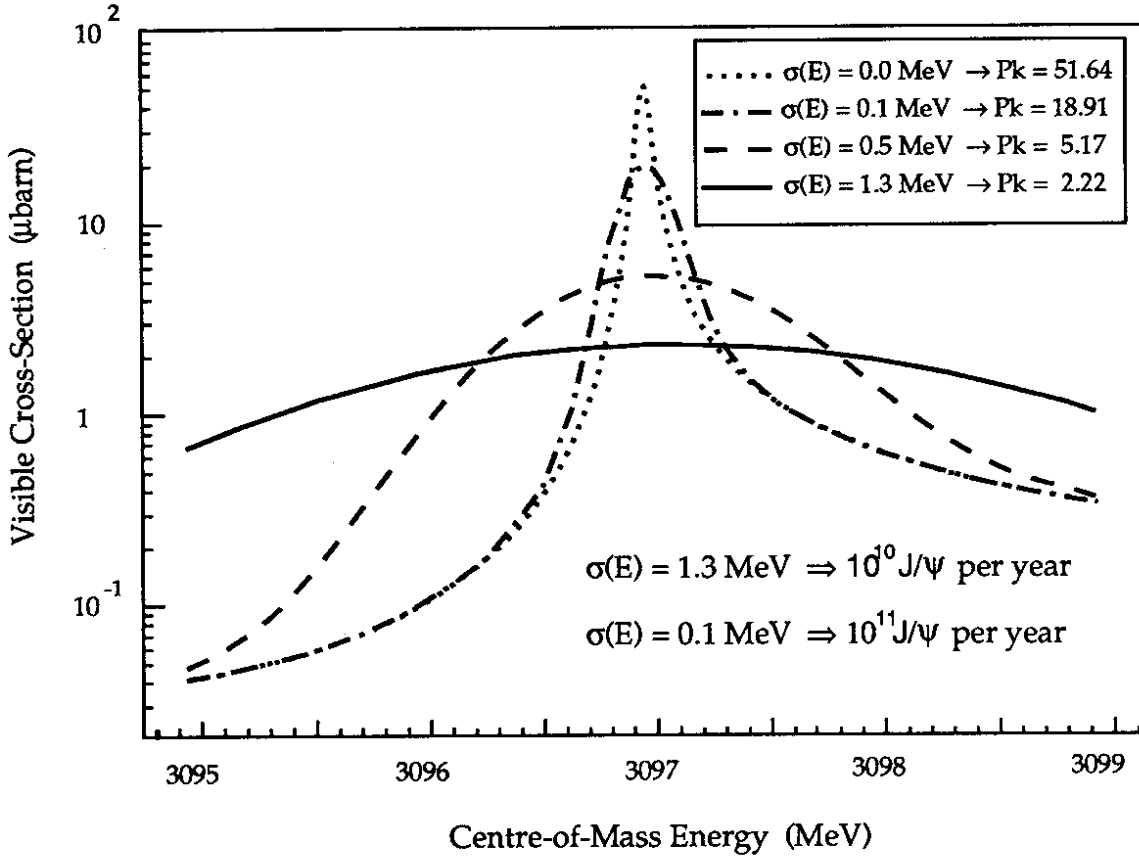


Figure 11: The observed J/ψ cross-section for various values of the collision energy spread $\sigma(E)$ [71].

the τ -charm Factory could be used to study many hadronic decays of these states[70]. The τ -charm Factory could also study the properties of the barely-known 1P_1 and η'_c states.

3.3.2 WEAK DECAYS AND AXIONS

The very high statistics and the narrow width of the J/ψ may provide the first opportunity to measure weak decays of a vector meson, such as $J/\psi \rightarrow D_s e \nu_e$ ($\text{Br} \simeq 10^{-8}$), or the C-violating decay $J/\psi \rightarrow \phi\phi$ ($\text{Br} \simeq 10^{-8}$). The J/ψ can be tagged via $\psi' \rightarrow \pi^+\pi^- J/\psi$ to allow searches for rare processes involving $J/\psi \rightarrow$ “nothing”.

Axions or other evasive neutrals can be produced in $J/\psi \rightarrow \gamma X$. The signature for such a decay is a single photon in the final state. The limiting factor here will be backgrounds from events with 3 photons in which only one photon is detected. Assuming the photon detection efficiency is 99%, the expected sensitivity is $\text{Br}(J/\psi \rightarrow \gamma X) \simeq 10^{-8}$.

3.3.3 CP VIOLATION

Since its discovery almost 30 years ago, CP violation has proved extremely difficult to observe in any system other than $K^0\bar{K}^0$. According to the Standard Model, CP-violating effects are indeed expected to be difficult to observe elsewhere, due to either small effects or small branching ratios to the relevant final states. However in order to understand the origin

of CP violation, it is vital to continue to search for more experimental information—and especially to search in new systems.

Recent studies[71, 72] have shown that it may be possible to observe direct CP violation by measuring differences in the decay parameters of hyperons (Y) and anti-hyperons (\bar{Y}) produced in $e^+e^- \rightarrow J/\psi \rightarrow Y\bar{Y}$. These processes are described by three parameters: Γ (decay width), α (asymmetry parameter) and β (parameter related to the transverse polarization of the daughter baryon). The CP-odd parameters, which are all zero if CP is conserved, are

$$\Delta_Y = \frac{\Gamma_Y - \Gamma_{\bar{Y}}}{\Gamma_Y + \Gamma_{\bar{Y}}}, \quad A_Y = \frac{\alpha_Y + \alpha_{\bar{Y}}}{\alpha_Y - \alpha_{\bar{Y}}}, \quad \text{and} \quad B'_Y = \frac{\beta_Y + \beta_{\bar{Y}}}{\alpha_Y - \alpha_{\bar{Y}}}.$$

The Standard Model predictions have large uncertainties coming from the top mass, the values of the CKM matrix elements and, most importantly, from model dependencies[73]. The expected range of values for the parameters is within an order-of-magnitude of the following[73]:

$$\Delta_Y \simeq 10^{-5}, \quad A_Y \simeq 10^{-4}, \quad \text{and} \quad B'_Y \simeq 10^{-3}.$$

The most studied parameter is A . Δ (which is constrained to be zero by CPT conservation) is the easiest to measure but it has the lowest sensitivity, and B' is the most difficult to measure but it has the highest sensitivity. Currently the best results have been obtained by PS185 (LEAR) with 10^4 $p\bar{p} \rightarrow \Lambda\bar{\Lambda}$ events, quoting $A_\Lambda = 0.024 \pm 0.057$ [74].

At the τ -charm Factory, CP violation may be measured in the processes

$$J/\psi \rightarrow \Lambda \bar{\Lambda} \rightarrow (p\pi^-) (\bar{p}\pi^+), \quad \text{and}$$

$$J/\psi \rightarrow \Xi^- \Xi^+ \rightarrow (\Lambda\pi^-) (\bar{\Lambda}\pi^+) \rightarrow (p\pi^- \pi^-) (\bar{p}\pi^+ \pi^+)$$

In the case of Λ decay, the α_Λ parameter is determined from the angular distribution of the proton in the Λ rest frame:

$$W(\theta) = 1 + \alpha_\Lambda \cos \theta$$

where θ is the polar angle of the proton with respect to the Λ polarization direction. In the case of Ξ decay, the α_Ξ parameter is determined in an analogous way from the angular distribution of the daughter Λ . However, in addition, there is now the possibility to measure the transverse polarization of the daughter Λ (by observing its decay) and hence to determine β_Ξ .

The $\Xi^-\Xi^+$ channel is more difficult for $p\bar{p}$ experiments because, at the optimum energy for the measurement (a \bar{p} momentum of about 1.65 GeV/c), the cross-section is only 2 μb , compared with 60 μb for $\Lambda\bar{\Lambda}$. However, the $\Lambda\bar{\Lambda}$ and $\Xi^-\Xi^+$ rates are equal at the J/ψ , with branching ratios of approximately 10^{-3} .

The measurements at the τ -charm Factory will depend on whether or not the e^+e^- colliding beams are longitudinally-polarized (Section 4.2.5). In the case of unpolarized beams, the correlations between the two (Y and \bar{Y}) decay chains from a single parent J/ψ must be measured. In this way, A_Ξ and B'_Ξ can be determined and, by combining the $\Lambda\bar{\Lambda}$ and $\Xi^-\Xi^+$ measurements, A_Λ can also be determined.

With longitudinally-polarized beams, all the parameters can be measured from single decay chains. In this case, A_Λ can be measured directly from the $\Lambda\bar{\Lambda}$ channel; and A_Λ , A_Ξ and B'_Ξ can be measured from the $\Xi^-\Xi^+$ channel. These measurements have improved

sensitivities and lower systematic errors relative to those for unpolarized beams (for similar statistical samples).

A sensitivity of about 6×10^{-4} for both the A_Y and B'_Y parameters could be reached with 10^{11} J/ψ decays[71, 72]. These could be produced in one year with 100 keV monochromator optics (Fig. 11). The B'_Y parameter is expected to be at least 10 times larger than the corresponding A_Y , offering the possibility of reaching sensitivities with one year's data (with a monochromator) that are within the range of values expected in the Standard Model.

4 The Spanish τ -charm Factory

4.1 Introduction

Following the initial idea[1] and the first machine design[2, 3], interest in the τ -charm Factory developed at INP Novosibirsk, JINR Dubna, LAL-Orsay and SLAC, as well as in Spain. Further machine studies were carried out at SLAC[5, 75], LAL-Orsay[76], Moscow/Novosibirsk[12, 77], and CERN[78]—each confirming the feasibility of a τ -charm Factory reaching a peak luminosity of $10^{33} \text{ cm}^{-2} \text{ sec}^{-1}$ with modest extrapolations of present accelerator technologies.

There are advanced preparations for τ -charm Factory projects in Russia and in Spain. The former project involves a new accelerator complex, including a τ -charm Factory, which is planned at JINR Dubna[79], in collaboration with ITEP Moscow and INP Novosibirsk. The latter project is an international τ -charm Factory Laboratory in Spain, involving physicists from Spain, other European countries, and the United States.

The τ -charm Factory was promoted within the Spanish particle physics community and brought to the attention of the Spanish Authorities by J.A. Rubio. The total construction cost of the Laboratory (materials and personnel) is estimated to be 300 MCHF. Spain has offered to provide the major fraction of the funds and is seeking collaboration with CERN on the project. A final decision is expected in 1992, in which case the research activities could start in 1997. In the remainder of this paper, we provide an overview of the designs of the machine and detector for the τ -charm Factory Laboratory in Spain (Figs. 12 and 13).

4.2 Accelerators

The τ -charm Factory is conceived as a single integrated experimental device consisting of an injector, a double-ring collider and a detector. The main operating range of the e^+e^- collider is 3-5 GeV total energy, with a peak luminosity of $10^{33} \text{ cm}^{-2} \text{ sec}^{-1}$ at 4 GeV. The accelerator complex is shown in Fig. 14. In this layout, newly-injected beam must make almost a full turn before reaching the interaction region, thereby minimizing detector backgrounds during injection.

4.2.1 COLLIDER

The collider operates with equal e^+ and e^- beam energies, up to a maximum of 2.5 GeV. A parameter list¹ for the collider at its peak luminosity is shown in Table 4. Each of the two

¹prepared by J.M. Jowett

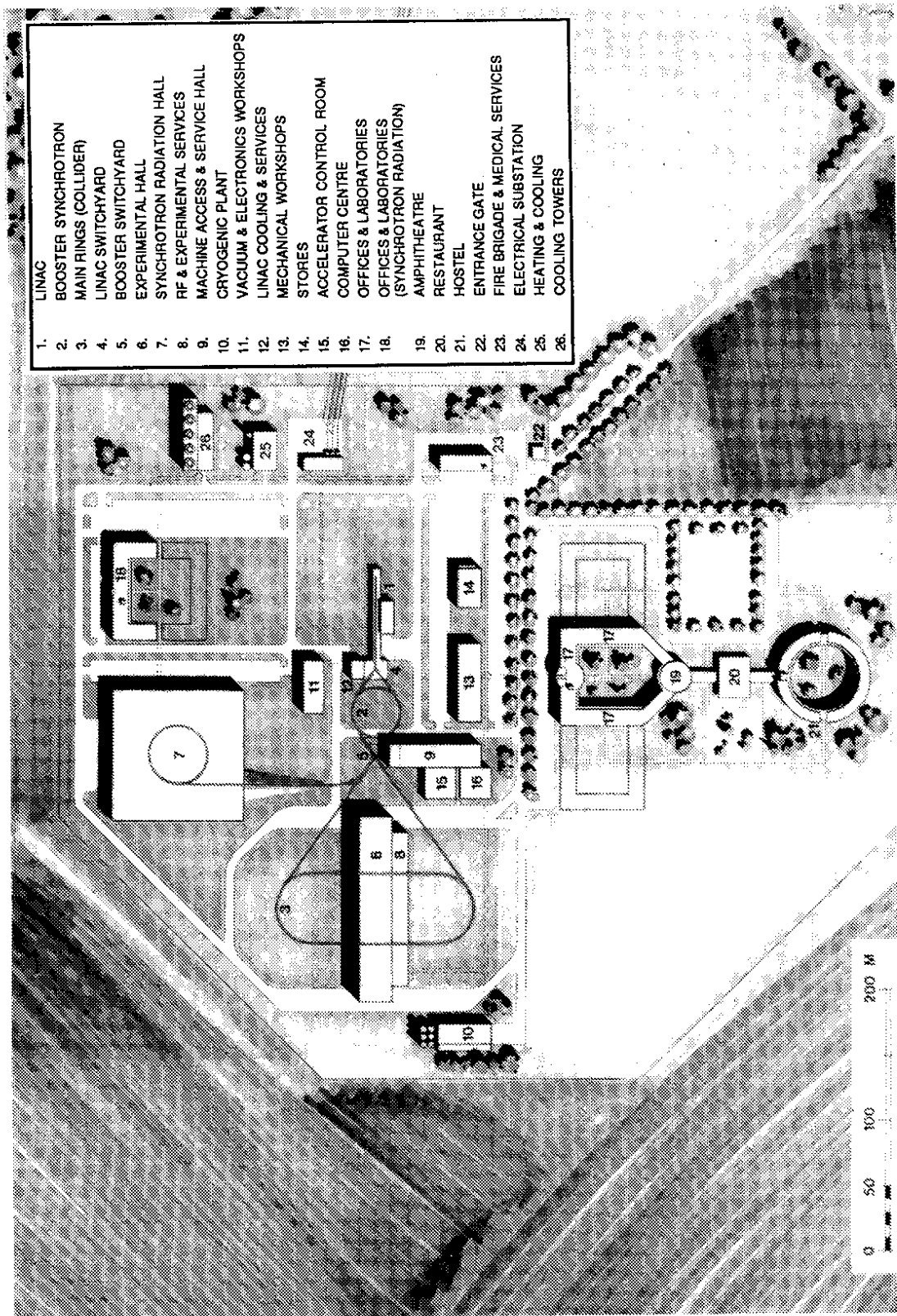


Figure 12: Plan view of the proposed 7-charm Factory Laboratory in Spain.

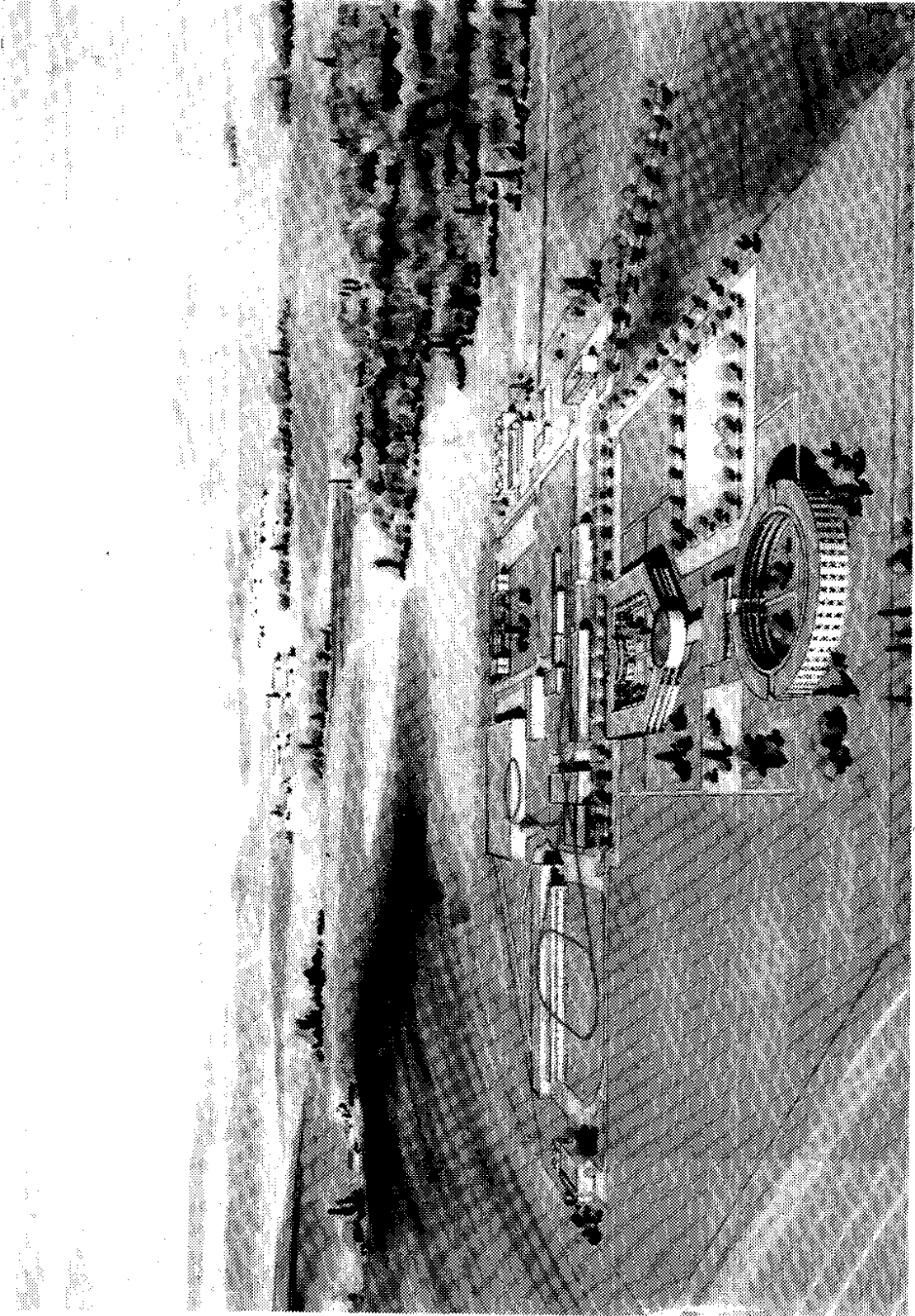


Figure 13: Perspective view of the proposed τ -charm Factory Laboratory in Spain.

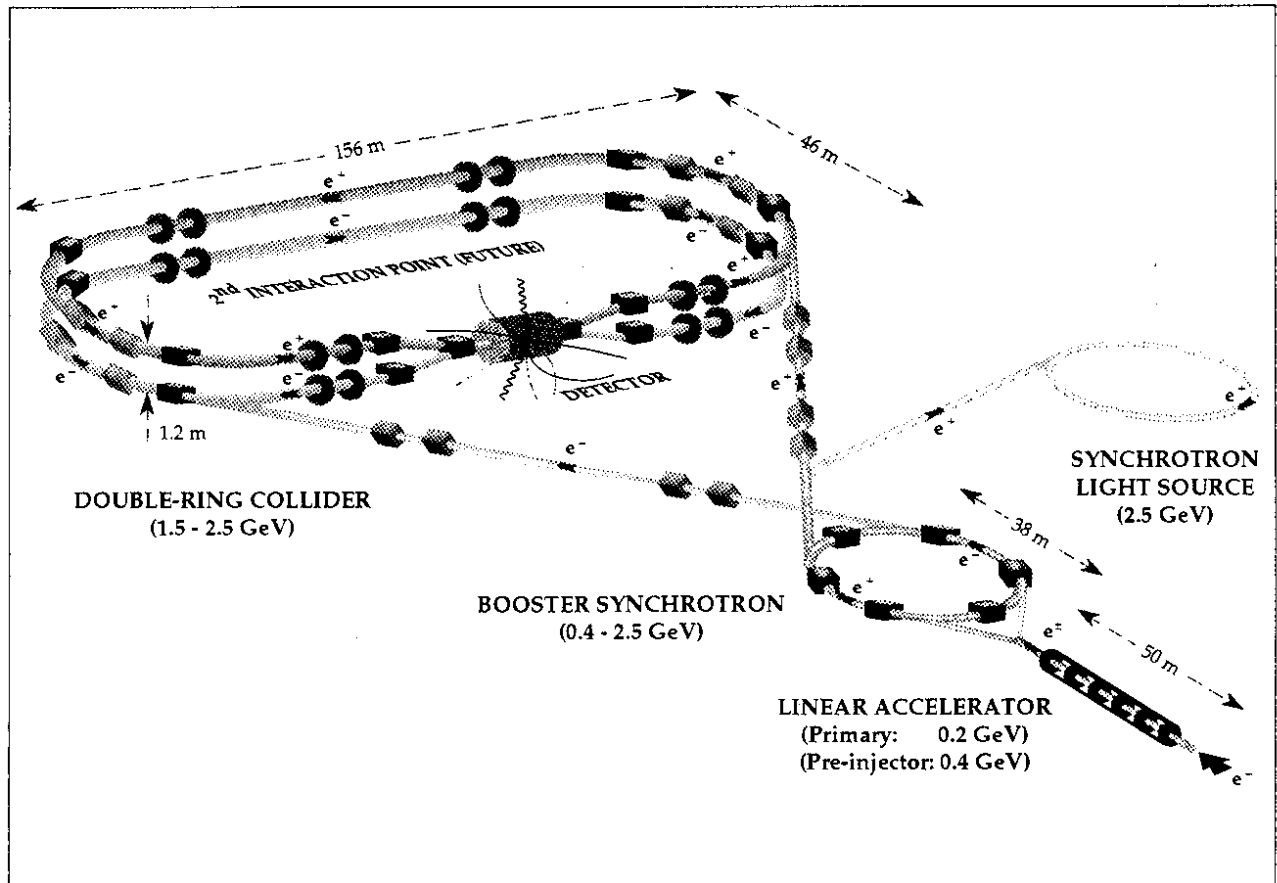


Figure 14: Schematic design of the τ -charm Factory Laboratory accelerator complex. The energy of each machine is indicated in parentheses.

rings consists of two conventional arcs and two long straight sections. The building blocks of the arcs are standard FODO cells and dispersion suppressors. The two rings merge in the experimental straight section, where the detector is located. The utility straight section on the opposite side of the ring contains special insertions for RF cavities, wigglers, etc., and provides considerable flexibility in tuning the collider, and in accommodating future upgrades.

The improvement in luminosity relative to previous machines at this energy (Table 5) is due to a higher stored current and tighter focusing at the interaction point. Although challenging, these parameters are within reach of present accelerator physics and technology. The high current is achieved with 30 e^+/e^- bunches distributed over the collider circumference of 360 m. Wigglers are used to maintain a large beam emittance (to permit high currents to be collided) over the full energy range. Parasitic crossings of the e^+ and e^- beams are avoided by vertical separation near the collision point and circulation of the beams in separate rings. The present design has a single interaction point. However, the possibility of a second interaction point is retained in the machine lattice in order to keep open the option for a second detector, should the physics case and experimental community emerge in the future.

Tight focusing of the beams ($\beta_y^* = 1$ cm) is achieved with superconducting $\mu\beta$ quadrupole

Energy	E	2	GeV
Circumference	C	360	m
Revolution frequency	f_0	832.76	kHz
Bending radius	ρ	10	m
β -function at IP	β_x^*	0.2	m
	β_y^*	0.01	m
Betatron coupling ($\epsilon_{yc}/\epsilon_{xc}$)	κ^2	0.05	
Betatron tunes	Q_x	10...	
	Q_y	11...	
Momentum compaction	α	0.0269	
Natural emittance	ϵ_x	272	nm
Fractional energy spread	σ_ϵ	5.04×10^{-4}	
Radiative energy loss per turn	U_0	132	keV
Radiation damping times	τ_x	45	msec
	τ_y	36	msec
	τ_ϵ	17	msec
Radiated power per beam	P_{rad}	75	kW
RF frequency	f_{RF}	400	MHz
RF voltage	V_{RF}	12.0	MV
Synchrotron tune	Q_s	0.124	
Number of bunches	k_b	30	
Bunch spacing	S_b	12	m
Bunch crossing frequency	f_b	25.0	MHz
Total current per beam	I	570	mA
Particles per bunch	N_b	1.42×10^{11}	
RMS bunch length	σ_z	6.26	mm
Longitudinal impedance ($\omega \rightarrow 0$)	$ Z/n _0$	$\simeq 1.3$	Ω
Longitudinal impedance (effective)	$ Z/n _{\text{eff}}$	$\simeq 0.20$	Ω
Beam-beam parameter	ξ_y	0.04	
Luminosity lifetime	τ_L	$\simeq 2$	hours
Luminosity	L	1.0×10^{33}	$\text{cm}^{-2}\text{sec}^{-1}$

Table 4: Parameter list for the τcF collider at its energy of maximum luminosity.

		SPEAR	BEPC	τ cF
Number of bunches	k_b	1	1	30
Effective bunch separation	S_b [m]	234	240	12
Total beam current	I [mA]	10	50	570
Vertical β -function at IP	β_y^* [m]	0.08	0.10	0.01
Beam-beam tune shift	ξ_y	0.025	0.04	0.04
Luminosity	L [$\text{cm}^{-2}\text{sec}^{-1}$]	1.0×10^{30}	1.0×10^{31}	1.0×10^{33}

Table 5: Comparison of e^+e^- colliders at $E_{beam} \simeq 2.0$ GeV. Recall that the luminosity, assuming optimum coupling, is $L = (I\gamma\xi_y/2er_e\beta_y^*) (1 + \sigma_y^*/\sigma_x^*)$. Since the beams are flat in these machines ($\sigma_y^* \ll \sigma_x^*$), the luminosity $L \propto (I\xi_y/\beta_y^*)E$.

magnets (possibly combined with permanent magnets) which approach to within 80 cm on each side of the collision point. Each of the two sets of $\mu\beta$ magnets is enclosed in a small superconducting solenoid which compensates the detector solenoid. Beyond these magnets are located 3.5 m-long electrostatic separators, followed by quadrupoles and septa, to separate the beams and direct them into their respective rings. The constraints associated with matching the vertical dispersion generated by the vertical bends accounts for the length of the insertion.

In order to benefit from the tight focusing, the bunch length must be small, $\sigma_z \lesssim \beta_y^*$. This is achieved with 6-8 single-cell superconducting RF cavities per ring, operating at 400 MHz and providing up to 12 MV accelerating voltage per ring. The specifications of these cavities are similar to those required for the LHC, so the frequency has been chosen with a view to a joint R&D programme. The circumference is chosen to allow maximum flexibility in the number of stored bunches both for the LHC RF frequency and for the more common 500 MHz.

The maximum stored beam current and, hence, the eventual luminosity of the τ -charm Factory is limited by single- or multi-bunch collective phenomena. Most of the technical challenges of the collider are associated first with the suppression of the sources of these instabilities and second, in the case of the multi-bunch instabilities, with the preparation of suitable feedback systems for their active correction. To avoid ‘‘turbulent’’ bunch lengthening of the short bunches in the τ -charm Factory, a low (effective) longitudinal impedance is required for the storage rings, $Z/n \simeq 0.2 \Omega$. This requires careful design of the vacuum chamber as well as the use of single-cell superconducting, rather than warm, RF cavities. Control of the multi-bunch instabilities—in which different bunches couple through the fields they leave behind in the cavities—will require the development of suitable higher-order-mode couplers to extract the trapped power from the RF cavities and will also require the installation of high-bandwidth feedback systems. Research towards such goals is under way at CERN and elsewhere. Finally, the electron ring has its own class of instabilities due to positive-ion trapping. These are handled by designing for the lowest-possible vacuum pressure and by installing low-impedance clearing electrodes along the vacuum chamber.

4.2.2 BACKGROUNDS AND MASKING

Preliminary studies have been made of synchrotron radiation, scattered beam particles and bremsstrahlung from the residual gas in the vacuum chamber, and masking in the interaction region[80].

Synchrotron radiation from the vertical bending magnets and quadrupoles in the interaction region has sufficiently low critical energies (≈ 0.35 keV) to allow simple masking and absorption in the beam-pipe to prevent significant detector backgrounds. (For example, the mean free path of a 1 keV photon is only $0.1 \mu\text{m}$ Fe.) The beam-pipe within 8 m of the interaction point is subject to an average heat load of 7 W/m (concentrated near the vertical plane) due to synchrotron radiation from the vertical-bend magnets. Suitable masking shields the cold beam-pipe in the region of the superconducting quadrupoles from this direct heat load. Care must also be taken to shield the electrostatic separator plates from synchrotron radiation, which could induce sparking and beam loss. If necessary, the plates could have a longitudinal slot to avoid the swath of synchrotron radiation.

Protection of the detector from bremsstrahlung and beam particles scattered by residual gas in the vacuum system requires adjustable masks upstream of the electrostatic separators, and between the separators and the quadrupoles. Simulations indicate that the rates will be mild: 6 kHz rate of electrons with $p_T \geq 100$ MeV/c strike the (6 cm-radius) beam-pipe within 80 cm of the interaction point, and most of these exit the ends of the detector at small radii. The flux of hard photons is comparable.

The arrangement of the RF cavities is asymmetric with respect to the main symmetry axes of the rings to ensure that each cavity is upstream of the nearby sources of synchrotron radiation (wigglers and arcs).

Protection of the interaction region during injection is helped by having each of the injection points as far from the interaction region as possible—about $3/4$ turn. One injection scheme under study is continuous synchrotron injection into the arcs to compensate for beam lifetime losses. Advantages include continuous data-taking at peak luminosity (the injected beam will have no transverse oscillation in the dispersion-free experimental straight section), and an injection system with potentially greater stability than one which operates for a few minutes every hour. A total of 16 adjustable collimators in the arcs are needed to protect the interaction region during injection. These collimators also create an aperture limit in both planes during physics running. Finally, as regards radiation damage to the detector during normal machine running, the radiation doses are well within safe limits.

4.2.3 INJECTOR

The injector chain is designed to fill the two rings at full energy in ≤ 10 min. In practice, the injection times will be shorter since the beams will be “topped-off” regularly to maintain a high average luminosity. Also there should be little setting-up time since the collider does not have to ramp or re-cycle its magnets between fills. The injector comprises a high intensity 200 MeV linac for e^+ production, followed by a 400 MeV linac and finally a 2.5 GeV, rapid-cycling (10 Hz) booster synchrotron.

4.2.4 DEDICATED SYNCHROTRON LIGHT SOURCE

The τ -charm Factory Laboratory will probably include an e^+ storage ring dedicated to synchrotron radiation studies. It would make use of the powerful positron injector which will be available during collider physics runs. The Spanish and European synchrotron radiation communities have recently endorsed the suitability of the τ -charm Factory Laboratory for such a light source, and indicated that the preferred energy is around 2.5 GeV.

4.2.5 FUTURE DEVELOPMENTS

Among the new accelerator ideas being considered for study at the τ -charm Factory is a monochromator optics which may reduce the spread in collision energies from $\simeq 1$ MeV to $\simeq 0.1$ MeV. Enough flexibility will be provided in the standard (high-emittance) optics to allow a future transition to a low-emittance monochromator optics with beams flattened in the *vertical* plane at the interaction point[12, 13, 14]. This would involve re-building the experimental insertion and inserting new quadrupoles in the free spaces foreseen for them in the arcs. As discussed previously, there is a strong physics interest in monochromator optics: tighter beam-energy constraints and D mass resolutions; increased rates at the J/ψ and ψ' ; and operation closer to $\tau^+\tau^-$ threshold, with correspondingly narrower monochromatic distributions and, in consequence, improved tagging of τ events, improved precision of branching ratio measurements, and improved sensitivity for decays such as $\tau \rightarrow eX$.

Another possibility under study is to use the second straight section for RF bunch rotation and non-zero crossing angles at the intersection point. If successful, such a “crab-crossing” optics may allow many more bunches to be stored, giving a large increase in luminosity.

Finally, the implementation of longitudinal beam polarization is also under study[13]. The polarization time in the collider is given by

$$1/\tau_{\text{pol}} \propto E^5 \int |B^3| ds.$$

With a mean bending field $|B| \simeq 0.6$ T in the standard optics, this indicates a long polarization time, $\tau_{\text{pol}} \simeq 3$ h. Since raising the bending field would have a negative impact on other aspects of the collider, an interesting alternative has recently been proposed[81] which separates the *generation* of the polarized beams from their *exploitation*. A high-field synchrotron in the injector chain would be used to (transversely) polarize the beams before injection into the collider. By using high-field (1.6 T) magnets, a short polarization time $\tau_{\text{pol}} \approx 10$ min could be achieved. Spin rotators in the injection lines leading to the collider would produce *longitudinally* polarized beams at injection. By including a solenoid spin corrector (of about 15 T-m at the J/ψ energy) in the second straight section of the collider, a longitudinal spin vector could be maintained at the interaction point. A polarimeter in the sloping part of the collider (near to the interaction point) measures the beam polarization. The long (de-)polarizing time in the bending field of the collider now becomes an advantage, although other de-polarizing effects need further study. The final result would be an extremely flexible choice of e^+e^- longitudinal spin alignment at the interaction point:

$$\rightarrow\rightarrow \quad \rightarrow\leftarrow \quad \leftarrow\leftarrow \quad \leftarrow\rightarrow$$

This choice could be made on a bunch-by-bunch basis, giving excellent control over systematic errors in the physics measurements.

	Mark III /BES	τ cF
Charged particles:		
Momentum resolution: $\sigma_p/p(\text{GeV}/c)$	$1.5\%p \oplus 1.5\%/\beta$ [MkIII] $0.7\%p \oplus 1.3\%/\beta$ [BES]	$0.3\%p \oplus 0.3\%/\beta$
p_{min}^π (MeV/c) for efficient tracking	80	50
Ω (barrel) ($\times 4\pi$ str.)	70%	90%
Photons:		
Energy resolution: $\sigma_E/E(\text{GeV})$	$17\%/\sqrt{E}$	$2\%/E^{1/4} \oplus 1\%$
Angular resolution: $\sigma_{\theta,\phi}$ (mr)	10 [MkIII] 5 [BES]	$5/\sqrt{E}$
2γ angular separation: $\Delta\theta_{2\gamma}$ (mr)	20	50
E_{min}^γ (MeV) for efficient detection	100	10
Particle identification:		
$h \rightarrow e$ rejection	4% at 0.5 GeV/c	0.1%
$h \rightarrow \mu$ rejection	5% at 1.0 GeV/c	$1\%/p(\text{GeV}/c) + 1\%$
$\pi \rightarrow K$ rejection	3σ at 0.7 GeV/c	3σ at 1.0 GeV/c
K_L^0/n detection efficiency	60%	95%
E_{min}^ν (MeV) for efficient ν tagging	-	$\simeq 100$

Table 6: Comparison of the performances of the Mark III (SPEAR), BES (BEPC), and τ cF detectors. The symbol ‘ \oplus ’ denotes addition in quadrature.

4.3 Detector

The improvement in the precision of experiments at the τ -charm Factory is due not only to a sharp increase in luminosity, but also to a substantial advancement in detector performance compared with previous experiments in the threshold region, such as Mark I, DASP, PLUTO, Mark II, DELCO, Crystal Ball, Mark III, and BES. A comparison of the performance of the τ cF detector with MarkIII/BES is made in Table 6.

The detector is presently being developed by a group² of approximately 100 experimental physicists from CERN, France, Germany, Portugal, Spain, the United Kingdom and other European countries, as well as the United States. The design brings together the best

²The τ -charm Factory physics and detector study group includes physicists from the following institutes: RWTH, Aachen (Germany); Univ. Aut. de Barcelona (Spain); Univ. Bochum (Germany); Univ. Cincinnati (USA); Univ. Coimbra (Portugal); Univ. Texas, Dallas (USA); Univ. Edinburgh (UK); CERN, Geneva (Switzerland); Univ. Glasgow (UK); Univ. Granada (Spain); Univ. Hamburg (Germany); Univ. Heidelberg (Germany); LIP, Lisboa (Portugal); Univ. Liverpool (UK); Imperial Coll., Univ. London (UK); University Coll., Univ. London (UK); CIEMAT, Madrid (Spain); Univ. Mainz (Germany); Univ. Manchester (UK); CNRS-Luminy, Marseille (France); Massachusetts Inst. Tech. (USA); Univ. Munich (Germany); Univ. Oregon (USA); LAL-Orsay (France); École Polytechnique, Paris (France); Rutgers Univ., New Brunswick (USA); Univ. Rome (Italy); Univ. California, Santa Cruz (USA); Univ. de Cantabria, Santander (Spain); Univ. de Santiago de Compostella (Spain); Univ. de Sevilla (Spain); SLAC, Stanford (USA); CRN Strasbourg (France); Univ. Illinois, Urbana-Champaign (USA); IFIC Valencia (Spain); Univ. Washington, Seattle (USA) and Univ. Zaragoza (Spain).

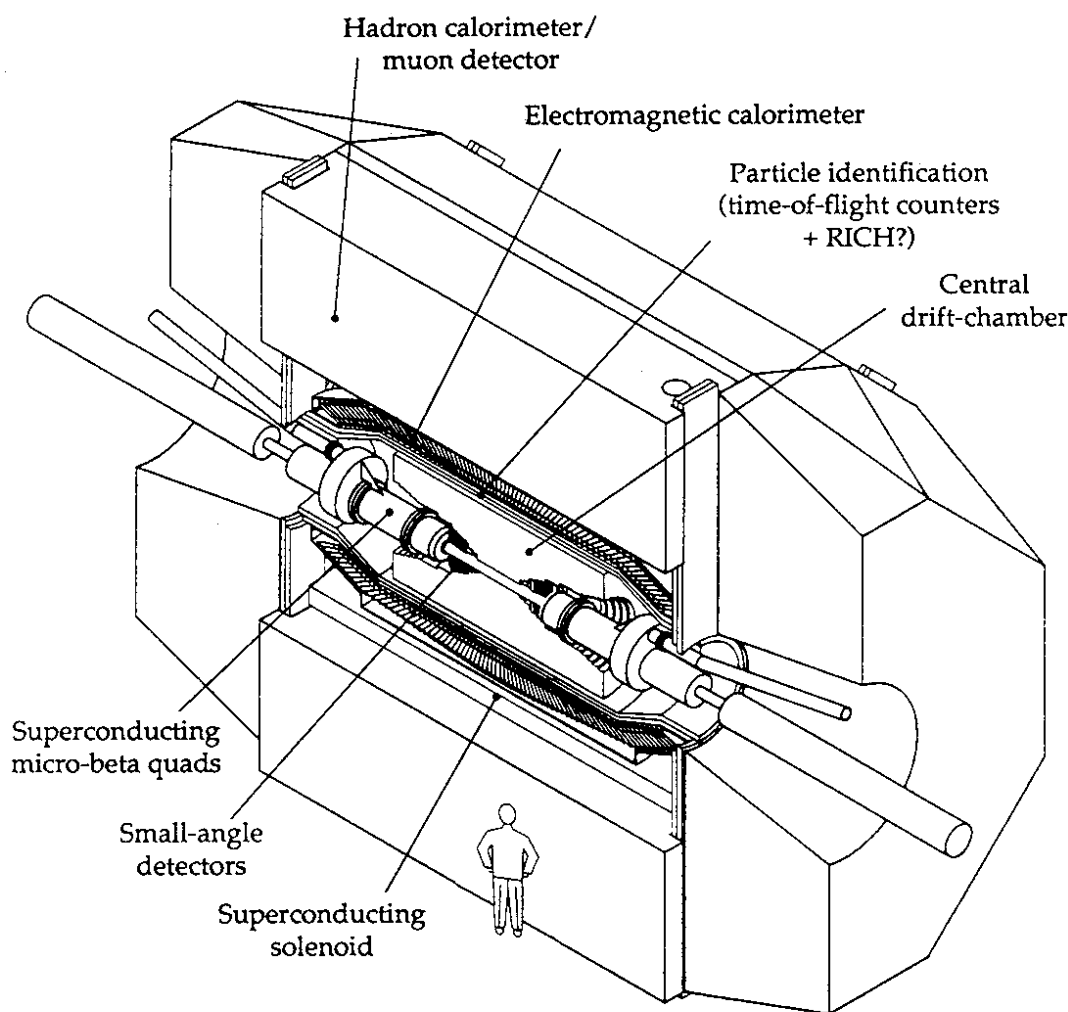


Figure 15: Perspective view of the τ -charm Factory detector. The primary rôle of the hadron calorimeter is to tag the presence of K_L^0/n , and not the traditional one of hadron energy measurement.

features of previous detectors into one device. In particular, it represents the first detector at these energies with high-resolution charged *and* neutral measurements, and with complete hermeticity, to allow missing ν 's to be tagged. Despite the novel design, however, most of the detector components are well understood and the detector should readily achieve its design performance.

The physics requirements on the τ cF detector design were evaluated during studies and discussions at the SLAC workshop[5]. These studies, together with further work reported at the Sevilla meeting[7] and at the CERN mini-workshops[8], have lead to the preliminary design of a detector and its computing system that should meet the physics requirements. This detector (Figs. 15 and 16) is briefly described below:

Magnet. Magnetic analysis of charged tracks is provided by a superconducting solenoid of field strength $\simeq 1.2$ T. The dimensions of the cryostat are: inner diameter 3.1 m, outer diameter 3.6 m, and length 5.8 m. The stored energy is 33 MJ.

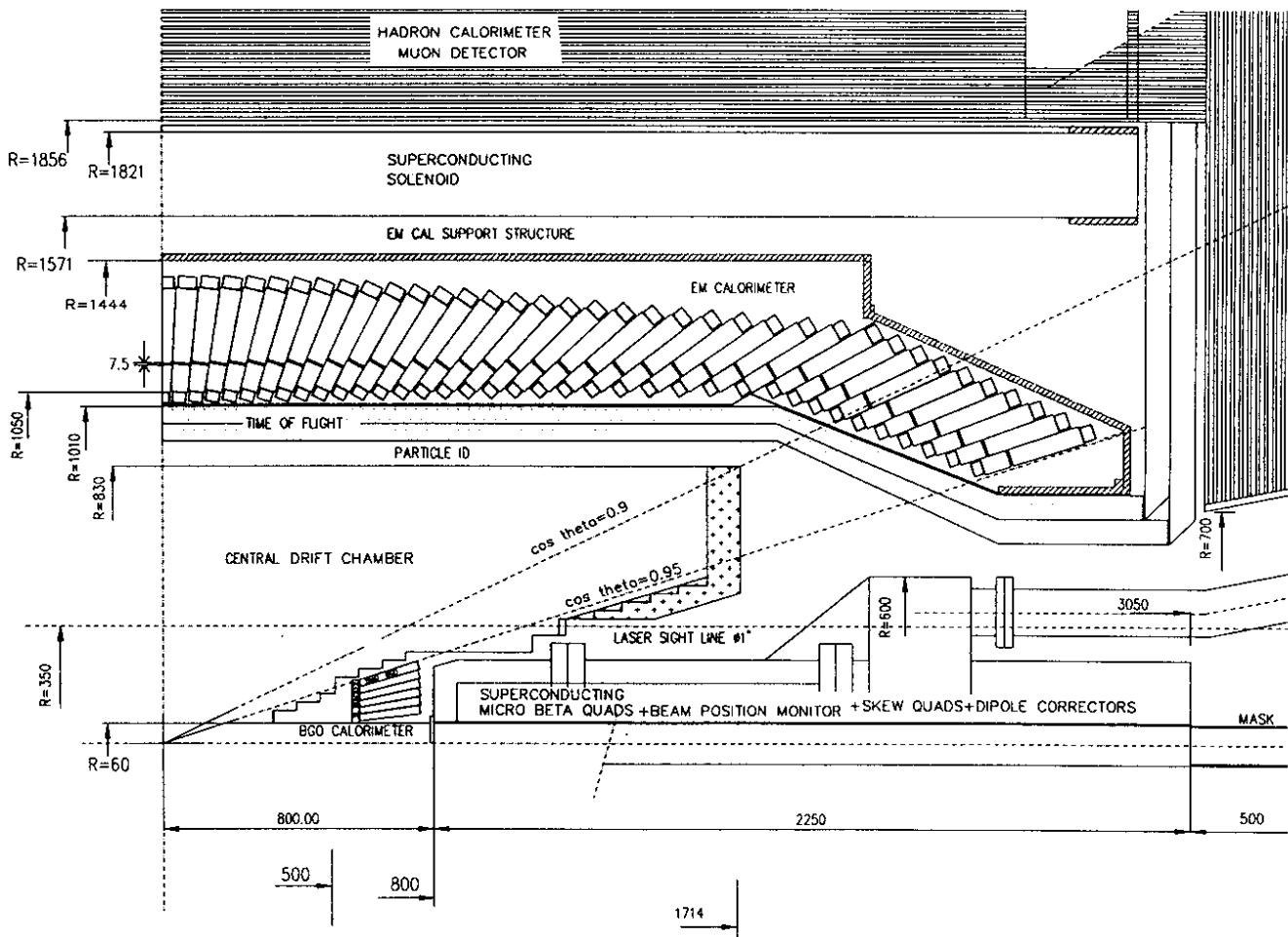


Figure 16: Side view of the inner part of the τ -charm Factory detector.

Tracking detector. The current design foresees a drift-chamber tracking detector extending over the radial range $6 \rightarrow 83$ cm. Measurement of the z coordinate is done by narrow-angle stereo since this is compatible with the low-gain requirements of dE/dx measurements. There are 40 anode wire hits per track ($\sigma_{x,y} = 150 \mu\text{m}$) which are arranged in superlayers, each containing 4 (uv) or 6 (z) anode wires. The maximum wire length is 3.2 m and the maximum drift distance is 2.4 cm, to minimize diffusion and pileup. There are a total of 2800 sense wires.

The design performance for the multiple Coulomb scattering term, $\sigma_p/p = 0.3\%/\beta$, places severe constraints on the amount of material that can be tolerated in the drift chamber. In order to achieve this performance, it is planned to use Al field-shaping wires and a He-based gas (e.g. He:CO₂:iso-C₄H₁₀ in the ratio 78:15:7).

In order to provide a large region of optimal performance, the tracking detector has an extended barrel region that subtends $90\% \times 4\pi$ str., leaving small end-caps that cover only $5\% \times 4\pi$ str. The end-caps are designed to be continuous with the barrel in order to avoid any loss of hermeticity. The inner face of each of the cryostats for the $\mu\beta$ quadrupole magnets is also instrumented, as described below, bringing the total detector coverage to $99.7\% \times 4\pi$ str.

Time-of-flight (ToF) counters. Since the kinematic limit of particles from τ or D decays is $\simeq 1$ GeV/c, sufficient identification of π , K, and p can be made by a combination of ToF and of dE/dx in the tracking detector. Useful (3σ) separation at 1 GeV/c requires a timing resolution of 120 ps over the (≥ 95 cm) flight path of the τ cF detector (Fig. 17). This performance can be achieved with two independent layers of plastic scintillator, each providing $\sigma_{\text{ToF}} = 170$ ps. It is proposed to install 128 counters per layer—probably made from 2 mm-diameter plastic scintillating fibres (SCIFI)[82, 83]—each of about 4 m length and cross-section 5×5 cm². As well as their superior timing properties, SCIFI counters have the advantage that they can be shaped to provide continuous coverage of both the barrel and end-cap regions (see Fig. 16).

It is foreseen to leave extra space between the drift chamber and the ToF counters to allow for future developments of particle-identification detectors. One possibility is a fast RICH[84] using either a solid NaF or liquid freon (C₆F₁₄) radiator. If a compact, low-mass RICH could be developed, it would substantially improve the πK , πe and $\pi\mu$ separations in the τ cF detector (compare Figs. 17 and 18).

Electromagnetic calorimeter. The electromagnetic calorimeter comprises an array of CsI(Tl) (or CsI(Na)) crystals arranged in a tower geometry that projects, with a small offset, towards the interaction point. There are a total of about 10 k towers, each with an entrance face $\simeq 5 \times 5$ cm² and a total depth of $16X_0$. The total volume of CsI(Tl) is about 10^4 l. The crystals are divided longitudinally into a front section of $\simeq 4X_0$ depth and a rear section of $\simeq 12X_0$. Each of the rear crystals is read out with two Si photodiodes (to provide redundancy) mounted on a waveshifter-plate that covers the rear face. A similar readout is provided at the front face of each of the front crystals. Longitudinal segmentation will provide improved rejection of fake γ 's from neutron albedo, as well as depth information to aid πe separation. Several ways are being investigated to improve the angular resolution of the calorimeter. These include the possibility of a position-measuring layer (Si wafer) between each front and rear pair of crystals, and finer transverse segmentation and readout of the front crystals.

Hadron calorimeter/ μ detector. Situated outside the solenoid is a fine-grained hadron calorimeter whose functions are to tag the presence of K_L^0/n , to identify μ , and to provide a flux return path. This has a perpendicular depth of $5.7\lambda_{abs}$ and is made from 76×1.0 cm Fe plates. The total Fe weight is about 1500 t. The plates are separated by gaps of 2 cm which contain drift chambers with wide drift cells (10-20 cm). Careful attention is paid to avoid cracks and other inefficient regions in the calorimeter that point to the origin.

The separation of π/K from μ is achieved by a combination of precise range-energy measurement, absence of interactions, and absence of an identifiable decay kink in the tracking chamber. Time-of-flight is used to identify μ below the minimum range of the calorimeter (250 MeV/c).

Small-angle detectors. The inner face of each $\mu\beta$ quadrupole cryostat is instrumented with a dense calorimeter— $16X_0$ BGO—preceded by a Si tracking detector. Each crystal tower has a front face $\simeq 2 \times 2$ cm² and is segmented in depth ($\simeq 4X_0 + 12X_0$). A position-measuring layer—based on a Si wafer with 5×5 mm² pads—may be inserted between the front and back crystals of each tower. The small-angle detectors complete

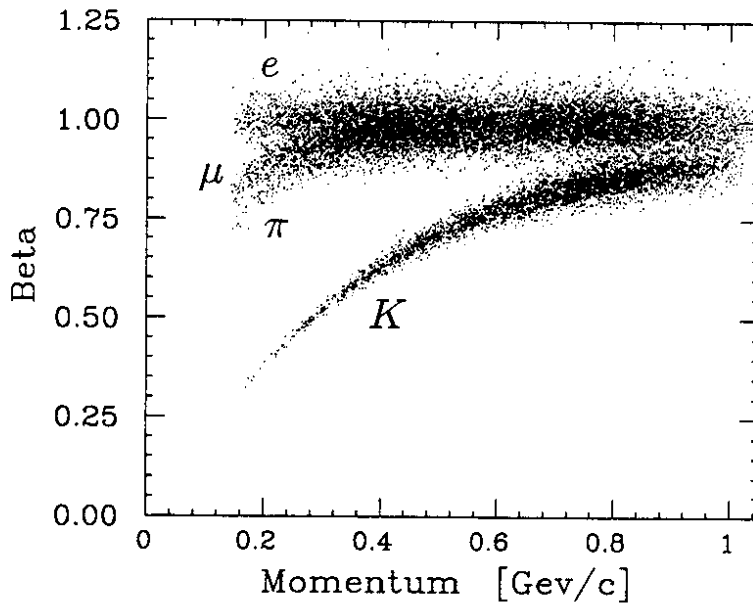


Figure 17: Time-of-flight particle separation in the τcF detector ($\sigma_{ToF} = 120$ ps (two layers) and minimum flight path = 0.95 m).

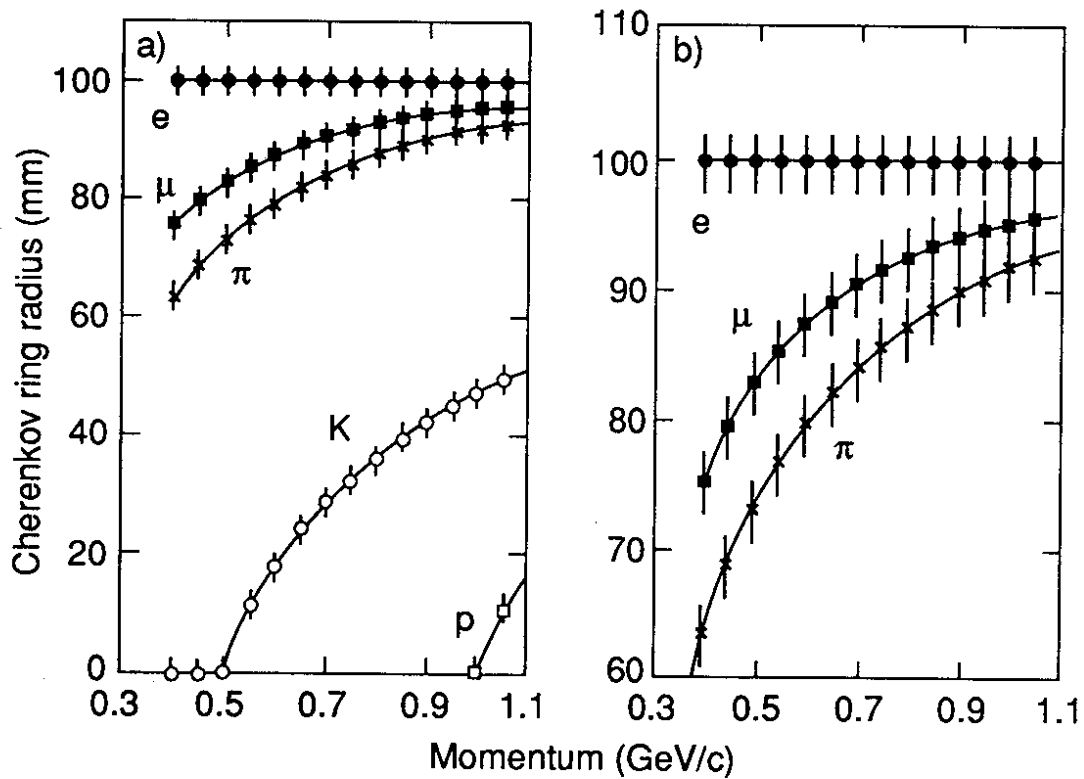


Figure 18: Fast RICH particle separation in the momentum range below 1.1 GeV/c, calculated from the measurements of ref. [84]. Figure b) provides an expanded vertical scale. The error bars indicate the 1σ measurement error on a single Cerenkov ring. The RICH has a 10mm-thick NaF radiator, a mean of about 20 photo-electrons per ring, and a total depth of 10 cm.

the solid angular acceptance and provide the luminosity monitor—both for the detector and for the feedback system that maintains beam alignment.

Trigger and data-acquisition system. In order to achieve a high rejection rate for unwanted events, a multi-level and pipelined approach to the triggering and data acquisition is required. A fast level 1 interaction trigger uses ToF counter signals and an analogue sum of the electromagnetic calorimeter energy. This should reduce the beam crossing rate of 25 MHz to a trigger rate of $\mathcal{O}(10\text{ kHz})$ —largely composed of background processes such as cosmic rays, synchrotron photons, beam-wall interactions, etc. A level 2 hardware trigger then makes more detailed event selection, based on charged tracks that emerge from the interaction volume and on neutral energy clusters in the electromagnetic calorimeter. The output rate of the level 2 trigger is expected to be equal to the actual physics event rate plus a background rate of $\mathcal{O}(1\text{ kHz})$ —largely beam-gas/wall interactions. The physics event rate is between $\simeq 50\text{ Hz}$ (off-resonance) and $\simeq 1\text{ kHz}$ (at the $J/\psi(3.10)$ and $\psi'(3.69)$).

Following a decision to accept an event by the level 2 trigger, detector information is transferred in digitized form to a large network of microprocessors with a computing power of about 10 k Mips, which constitute the level 3 software trigger. These processors first repeat the level 2 event selection criteria with full detector resolution, in order to filter out the residual background events. A full event analysis is then carried out to select interactions with the desired physics characteristics. The selected and compressed events are then recorded on magnetic cassettes at a rate of 50-100 Hz.

The τ -charm Factory will generate an enormous amount of data; the storage requirements are up to 10 Tbytes per year, of which a large fraction must be available at the Laboratory on disks (for fast random access). Although these computer and storage requirements are large, it is expected that there will be substantial commercial progress on the timescale of the project. High-speed networks will allow remote analysis and event filtering by the collaborating teams from their home institutes. The selected subsets of data are then written onto cartridges and transported to the computer centres of the home institutes for physics analyses.

5 Conclusions

Recent results from LEP and SLC indicate that only three families of fundamental fermions may exist in Nature. These results indicate the need for higher-precision studies to be made of the known fermions, in searches of a deeper understanding of the Standard Model and of clues to its extensions. In future, significant progress in this direction will require dedicated machines—particle factories—that are optimized for the study of specific particles.

The τ -charm Factory is the pre-eminent accelerator to explore the τ and ν_τ leptons, and the charm quark. Through decays of the J/ψ , the τ -charm Factory also addresses many important questions that remain at lower energies, including gluonium spectroscopy and CP violation in hyperon decays. As well as providing the largest data samples, the threshold region offers unique control of systematic errors. This is due to several features that are available only near threshold: exceptionally low backgrounds, which can be measured experimentally; the ability to produce τ 's and D 's nearly at rest, which results in monochromatic

particles from two-body decays; small radiative corrections; minimal overlap of final-state particles; the existence of high-rate sources for experimental calibration and monitoring of the detector; and excellent mass resolutions and particle identification. In addition, the τ -charm Factory is the only machine that can single-tag τ^\pm , D^0 , D^\pm and D_s^\pm . Single-tagged data samples will allow unbiased studies to be made under clean background conditions and without any flux uncertainties. Together, these features provide a unique experimental environment for this physics.

Independent machine studies at CERN, LAL-Orsay, Novosibirsk and SLAC have concluded that a luminosity of $10^{33} \text{ cm}^{-2} \text{ sec}^{-1}$ is feasible for an e^+e^- collider operating near $\tau^+\tau^-$ threshold. This is an improvement by 2-3 orders of magnitude over previous machines at these energies. Several future upgrades of the collider are under study which would extend the physics sensitivity; they include monochromator optics and longitudinal beam polarization. In addition to the large improvement in machine performance, the proposed τ -charm Factory detector is far more sensitive than previous detectors in the τ -charm threshold region, combining high-resolution charged and neutral measurements with complete hermeticity and the capability of tagging missing ν 's. The combined τ -charm Factory collider and detector create an unprecedented experimental tool for τ and charm physics.

Spain is proposing to build an international τ -charm Factory Laboratory and is seeking collaboration with CERN on the project. A final decision is expected in 1992 and we can look forward to the first colliding beams in 1997.

Acknowledgements

I would like to thank Jose Valle, Jorge Velasco and the Universidad Internacional Menéndez y Pelayo (Valencia) for hosting a most enjoyable meeting. I am indebted for many ideas and discussions to my colleagues in Europe and the United States who are developing the τ -charm Factory. I would like, in particular, to acknowledge the co-authorship of parts of this paper with Michel Benot, Alvaro de Rújula, Enrique González, John Jowett, Julio Oropesa, Antonio Pich, Juan Antonio Rubio and Carlos Willmott.

References

- [1] J. Kirkby, *A τ -charm Factory at CERN*, CERN-EP/87-210 (1987), and Proc. International School of Physics with Low-Energy Antiprotons; Spectroscopy of Light and Heavy Quarks, Erice, Sicily, 1987 (Plenum Press, New York, 1989) 401.
- [2] J.M. Jowett, *Initial design of a τ -charm Factory at CERN*, CERN LEP-TH/87-56 (1987).
- [3] J.M. Jowett, *The τ -charm Factory storage ring*, CERN-LEP/88-22 (1988), and Proc. 1st European Particle Accelerator Conference, Rome, 1988 (World Scientific, Singapore, 1989) 368.
- [4] M.L. Perl et al., *Evidence for anomalous lepton production in e^+e^- annihilation*, Phys. Rev. Lett. 35 (1975) 1489.
- [5] *Proc. Tau-Charm Factory Workshop*, SLAC, California, 23-27 May 1989, ed. L.V. Beers, SLAC-Report-343 (1989).

- [6] *Proc. Workshop on Tau Lepton Physics*, Orsay, France, 24-27 September 1990, eds. M. Davier and B. Jean-Marie (Editions Frontières, 1991).
- [7] *Proc. Meeting on the Tau-Charm Factory Detector and Machine*, Sevilla, Spain, 29 April-2 May 1991, eds. J. Kirkby and J.M. Quesada (Univ. Sevilla, to be published).
- [8] *Proc. Mini-workshops on the Tau-Charm Factory Physics, Detector and Computing*, CERN, Switzerland, October 1991 (in preparation).
- [9] A. Pich, *Tau physics*, CERN-TH.6237/91 (1991), to appear in "Heavy Flavours", Advanced Series on Directions in High Energy Physics, eds. A.J. Buras and M. Lindner (World Scientific, 1991).
- [10] R.H. Schindler, *Charmed meson physics accessible to a $10^{33} \text{ cm}^{-2} \text{ sec}^{-1} e^+e^-$ collider operating near charm threshold*, Proc. Les Rencontres de Physique de la Vallée d'Aoste, Italy, 1989, ed. M. Greco (Editions Frontières, 1989) 89.
- [11] M.B. Voloshin, *Topics in τ physics at a tau-charm factory*, Univ. Minnesota preprint TPI-MINN-89/33-T (1989).
- [12] Y. Alexakhin, A. Dubrovin and A. Zholents, *Proposal on a Tau-Charm Factory with monochromatization*, Proc. 2nd European Particle Accelerator Conference, Nice, France, v.1 (1990) 398.
- [13] J.M. Jowett, A. Zholents et al., paper submitted to the International Particle Accelerator Conference, Hamburg, Germany (1992).
- [14] A. Faus-Golfe and J. Le Duff, *A versatile lattice for a Tau-Charm Factory that includes a monochromatization scheme*, LAL-Orsay preprint LAL/RT 92-01 (1992).
- [15] J. Kirkby, *Tau physics prospects at a τ -charm Factory*, in [6], p. 453.
- [16] J.J. Gomez-Cadenas, *Lepton flavour violating processes involving τ leptons*, in [6], p. 349.
- [17] T. Skwarnicki, *Tau decays to multiphoton final states*, in [5], p. 519.
- [18] H. Harari and Y. Nir, *Bounds on neutrino masses from neutrino decay rates, cosmology and the see-saw mechanism*, Nucl. Phys. B292 (1987) 251.
- [19] E.W. Kolb et al., Phys. Rev. Lett. 67 (1991) 533.
- [20] A.G. Cohen, D.B. Kaplan and A.E. Nelson, Phys. Lett. B263 (1991) 86.
- [21] G.F. Giudice, Phys. Lett. B251 (1990) 460.
- [22] J.J. Gómez-Cadenas, *Beautiful τ physics in the charm land*, in [5], p. 48.
- [23] J.J. Gómez-Cadenas et al., Phys. Rev. D41 (1989) 2179.
- [24] J.J. Gómez-Cadenas, C.M. González García and A. Pich, Phys. Rev. D42 (1990) 3093.
- [25] H. Albrecht et al. (ARGUS), *An improved upper limit on the ν_τ mass from the decay $\tau^- \rightarrow \pi^- \pi^- \pi^- \pi^+ \pi^+ \nu_\tau$* , Phys.Lett. B202 (1988) 149.
- [26] W. Bacino et al. (DELCO), *Measurement of the threshold behaviour of $\tau^+\tau^-$ production in e^+e^- annihilation*, Phys.Rev.Lett. 41 (1978) 13.
- [27] Y.M. Shatunov and A.N. Skrinsky, *Polarized beams in storage rings and high precision measurements of particle masses*, Particle World 1 (1989) 35.

- [28] Y.S. Tsai, *Decay correlations of heavy leptons in $e^+e^- \rightarrow l^+l^-$* , Phys.Rev. D4 (1971) 2821.
- [29] F. Gilman and S.H. Rie, *Calculation of exclusive decay modes of the tau*, Phys.Rev. D31 (1985) 1066.
- [30] H.J. Behrend et al. (CELLO), Z.Phys. C46 (1990) 537.
- [31] D. Decamp et al. (ALEPH), *Measurement of tau branching ratios*, CERN-PPE/91-186 (1991), (submitted to Z.Phys.C.).
- [32] M. Danilov et al. (ARGUS), plenary talk at the LP-HEP91 Conference, Geneva, Switzerland (1991).
- [33] W.J. Marciano and A. Sirlin, *Electroweak radiative corrections to τ decay*, Phys. Rev.Lett. 61 (1988) 1815.
- [34] Y.S. Tsai, *Effects of charged Higgs in τ decay*, SLAC-PUB-5003 (1989), in [5], p. 387.
- [35] W. Fetscher, H.J. Gerber and K.F. Johnson, Phys. Lett. B173 (1986) 102.
- [36] W. Fetscher, *Leptonic τ decays: how to determine the Lorentz structure of the charged leptonic weak interaction by experiment*, Phys.Rev. D42 (1990) 1544, and in [6], p. 49.
- [37] H. Janssen et al., *The Michel parameter for the decay $\tau \rightarrow e\nu\nu$* , Phys.Lett. B228 (1989) 273.
- [38] A. Golutvin (ARGUS), *Determination of the Michel parameter in tau decay*, in [6], p. 171.
- [39] B.C. Barish, *Rare tau decays*, in [5], p. 113.
- [40] C.A. Heusch, *Looking for leptoquarks*, Proc. Les Rencontres de Physique de la Vallée d'Aoste, Italy, 1989, ed. M. Greco (Editions Frontières, 1989) 399.
- [41] A. Masiero, *Looking beyond the Standard Model in tau physics*, in [6], p. 333.
- [42] S. Kelley et al., *Exploring the chiral structure of lepton flavor violation*, CTP-TAMU-19/91 (1991).
- [43] M.C. Gonzalez-Garcia and J.W.F. Valle, *Supersymmetric signals in muon and tau decays*, Univ. Valencia preprint IFIC/90-56 (submitted to Nucl. Phys. B).
- [44] J. Hewett and T. Rizzo, Phys. Rep. 183 (1989) 193.
- [45] A. Pich, Phys. Lett. B196 (1987) 561.
- [46] K.K. Gan, *Multiple-neutral-meson decays of the τ lepton at a τ -charm Factory.*, in [5], p. 554.
- [47] E.W.N. Glover and J.J. van der Bij, *Rare Z decays*, in CERN 89-08, Vol. II (1989) 1.
- [48] A. de Rujula, *Physics at the τ -charm thresholds*, in [7].
- [49] J.W.F. Valle, *New physics in tau decays*, in [7].
- [50] J. Simpson, Phys. Rev. Lett. 54 (1985) 1891;
A. Hime and J. Simpson, Phys. Rev. D39 (1989) 1825;
A. Hime and N. Jelley, Univ. Oxford preprint OUNP-91-01 (1991).
- [51] B. Barbieri and L.J. Hall, Berkeley preprint LBL-30465 and UCB-PTH-91/13 (1991).

- [52] R. Alemany and J.J. Gomez-Cadenas, Univ. Aut. Barcelona preprint (in preparation).
- [53] S.M. Barr and A. Zee, *Electric dipole moment of the electron and of the neutron*, Phys. Rev. Lett. 65 (1990) 21.
- [54] J.A. Grifols and A. Méndez, Phys. Lett. B255 (1991) 611 [Erratum: B259 (1991) 512].
- [55] F. del Aguila and M. Sher, Phys. Lett. B252 (1990) 116;
S.M. Barr and W.J. Marciano, in *CP Violation* (Advanced Series on Directions in High Energy Physics - Vol.3), ed. C. Jarlskog, World Scientific (Singapore 1989).
- [56] W. Bernreuther and O. Nachtmann, Phys. Rev. Lett. 63 (1989) 2787 [Erratum: 64 (1990) 1072]; and *How to search for an electric dipole form factor of the τ lepton at a τ -charm Factory*, in [5], p. 545.
- [57] A. Pich, *Hadronic tau decays and QCD*, in [6], p. 321; and in [9].
- [58] I.I. Bigi, *$D^0 \bar{D}^0$ mixing and CP violation*, in [5], p. 169.
- [59] A. Seiden, *Physics summary τ -charm Factory Workshop*, in [5], p. 252.
- [60] G. Gladding, *$D^0 \bar{D}^0$ mixing and CP violation: experimental projections for a τ -charm Factory*, in [5], p. 169.
- [61] J.M. Izen, *Semi-leptonic charm decay at a τ -charm Factory*, in [5], p. 605.
- [62] D. Pitman, *D_s^\pm semi-leptonic decays at a τ -charm Factory*, in [5], p. 616.
- [63] P.C. Kim, *Pure leptonic decays of the D and D_s mesons*, in [5], p. 671.
- [64] M. Perl and R. Schindler, *The Tau-Charm Factory: experimental perspectives*, in [7].
- [65] R.S. Willey, *Rare decays of D mesons*, in [5], p. 196.
- [66] I.E. Stockdale, *A study of rare D decays for the Tau-Charm Factory*, in [5], p. 724.
- [67] W.H. Toki, *J/ψ and charmonium physics in a Tau-Charm Factory*, in [5], p. 207;
F.E. Close, *Exotic hadrons and hadron dynamics at a Tau-Charm Factory*, in [5], p. 220.
- [68] L. Kopke and N. Wermes, Phys. Rep. 174 (1989) 67.
- [69] F. Couchot, *Experimental search for gluonic mesons*, Proc. International School of Physics with Low-Energy Antiprotons; Spectroscopy of Light and Heavy Quarks, Erice, Sicily, 1987 (1989) 159;
G. Eichten, *Experimental status of J/ψ decays*, idem, p. 183.
- [70] R. Mir, *Open topics in charmonium physics*, in [5], p. 742.
- [71] E.M. González Romero, *CP violation study in the process $e^+e^- \rightarrow J/\psi \rightarrow \Lambda \bar{\Lambda} \rightarrow p\pi^- \bar{p}\pi^+$* , in [7].
- [72] E.M. González Romero and J.I. Illiana, *CP violation study in the processes $e^+e^- \rightarrow J/\psi \rightarrow \Lambda \bar{\Lambda}$ and $J/\psi \rightarrow \Xi^- \Xi^+$* , (in preparation).
- [73] X.G. He, H. Steger and G. Valencia, Phys. Lett. B272 (1991) 411.
- [74] P.D. Barnes et al., *Study of the reaction $p\bar{p} \rightarrow \Lambda \bar{\Lambda}$ at 1.546 and 1.695 GeV/c*, CERN-PPE/90-169 (1990).
- [75] B. Barish et al., *Tau-Charm Factory design*, SLAC-PUB 5180 (1990).

- [76] J. Gonichon, J. Le-Duff, B. Mouton and C. Travier, *Preliminary study of a high luminosity e^+e^- storage ring at a c.m. energy of 5 GeV*, LAL-Orsay preprint LAL/RT 90-02 (1990).
- [77] M.V. Danilov et al., *Complex of e^+e^- storage rings for investigation of charmed particles and tau-leptons (tau-charm factory)*, ITEP (Moscow) preprint 67-90 (1990).
- [78] Y. Baconnier et al., *A tau-charm factory laboratory in Spain combined with a synchrotron light source*, CERN/AC/90-07 (1990).
- [79] V.S. Alexandrov et al., *JINR Tau-Charm Factory design considerations*, Proc. IEEE Particle Accelerator Conference, San Francisco, 6-9 May 1991, Dubna preprint E9-91-178.
- [80] D. Stoker, *Backgrounds and masking at the Tau-Charm Factory*, in [7].
- [81] A. Zholents, private communication; and ref [13].
- [82] M. Kuhlen et al., *Timing properties of long scintillation counters based on scintillating fibres*, CALT-68-1648 (1990), submitted to Nucl.Inst.Meth.
- [83] H. Kichimi, *ToF counter for KEK B Factory*, Proc. Workshop on Physics and Detectors for KEK Asymmetric B-Factory, KEK, Tsukuba, Japan, 15-18 April 1991, eds. H. Ozaki and N. Sato, KEK Proceedings 91-7 (1991) 410.
- [84] R. Ribeiro et al., *Particle identification at the τ -charm Factory using a fast RICH detector*, in [7].